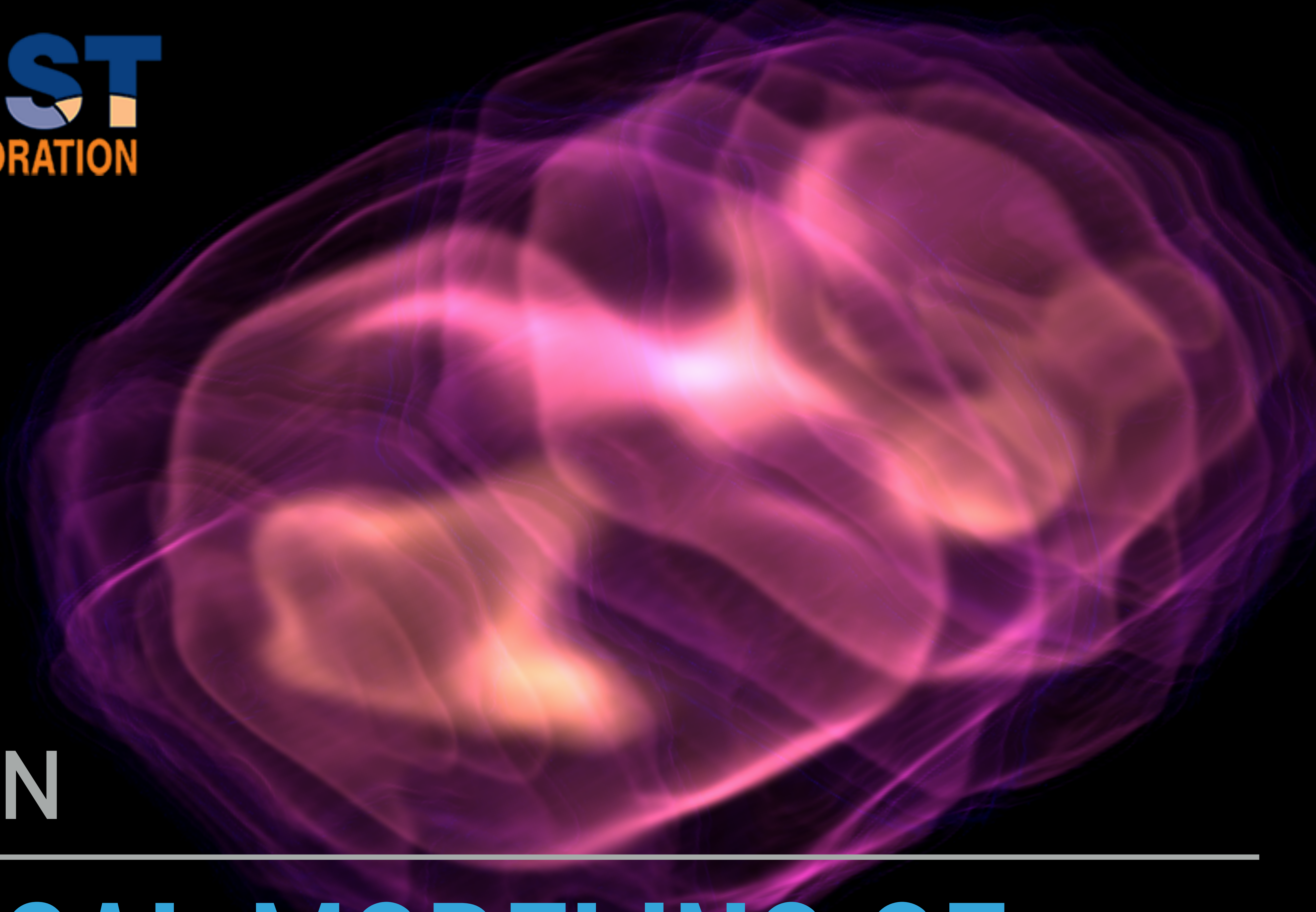

CHUN SHEN

DYNAMICAL MODELING OF BULK EVOLUTION AT RHIC BES

April 11 2019, Denver

APS GHP Meeting 2019

Phase diagram of hot nuclear matter

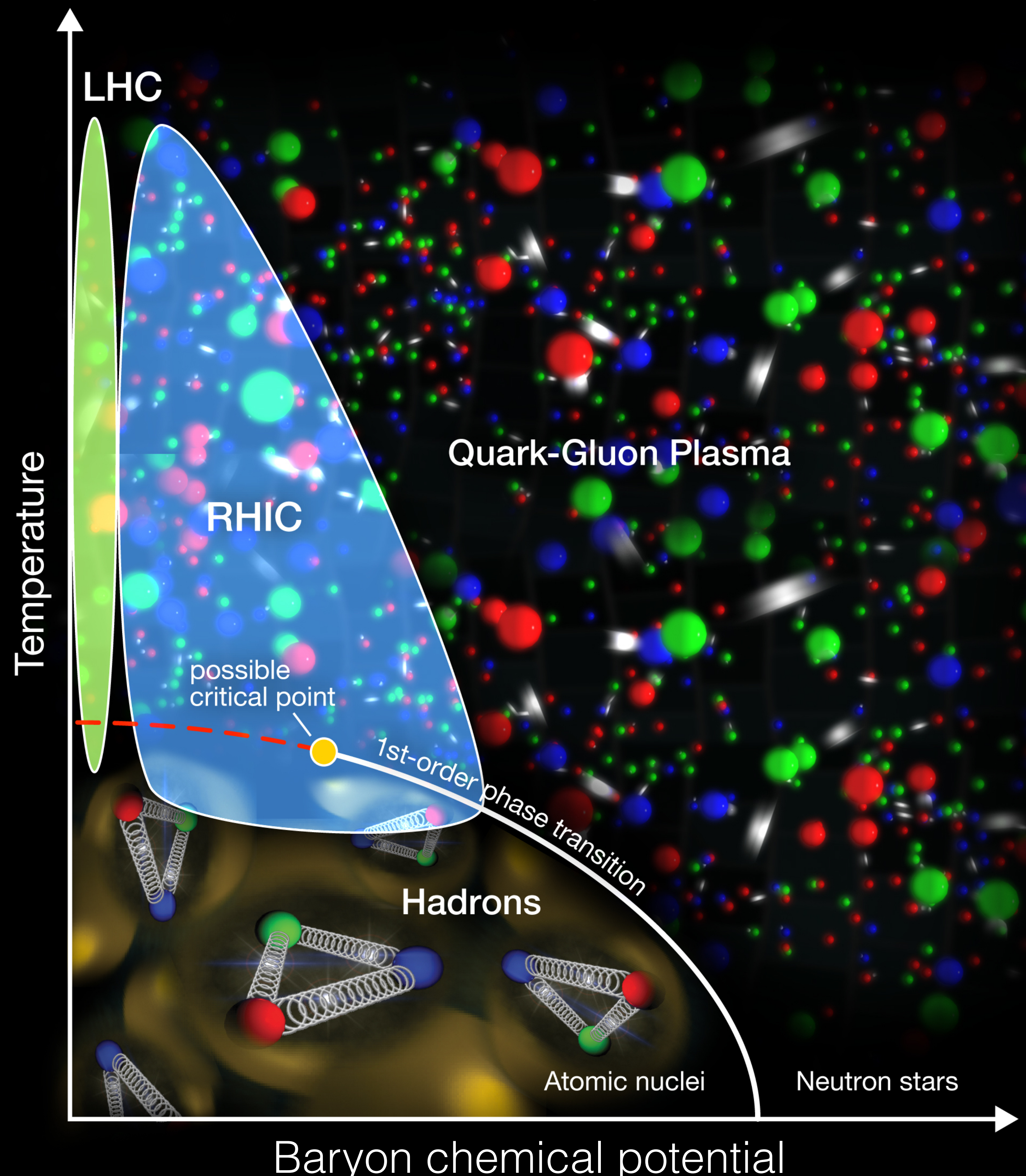

- What is the phase structure of nuclear matter
- What are the transport properties of the Quark-Gluon Plasma (QGP)
- Where is the critical point located

The picture is taken from http://www.bnl.gov/newsroom/news.php? a=11446

Multi-stage bulk evolution

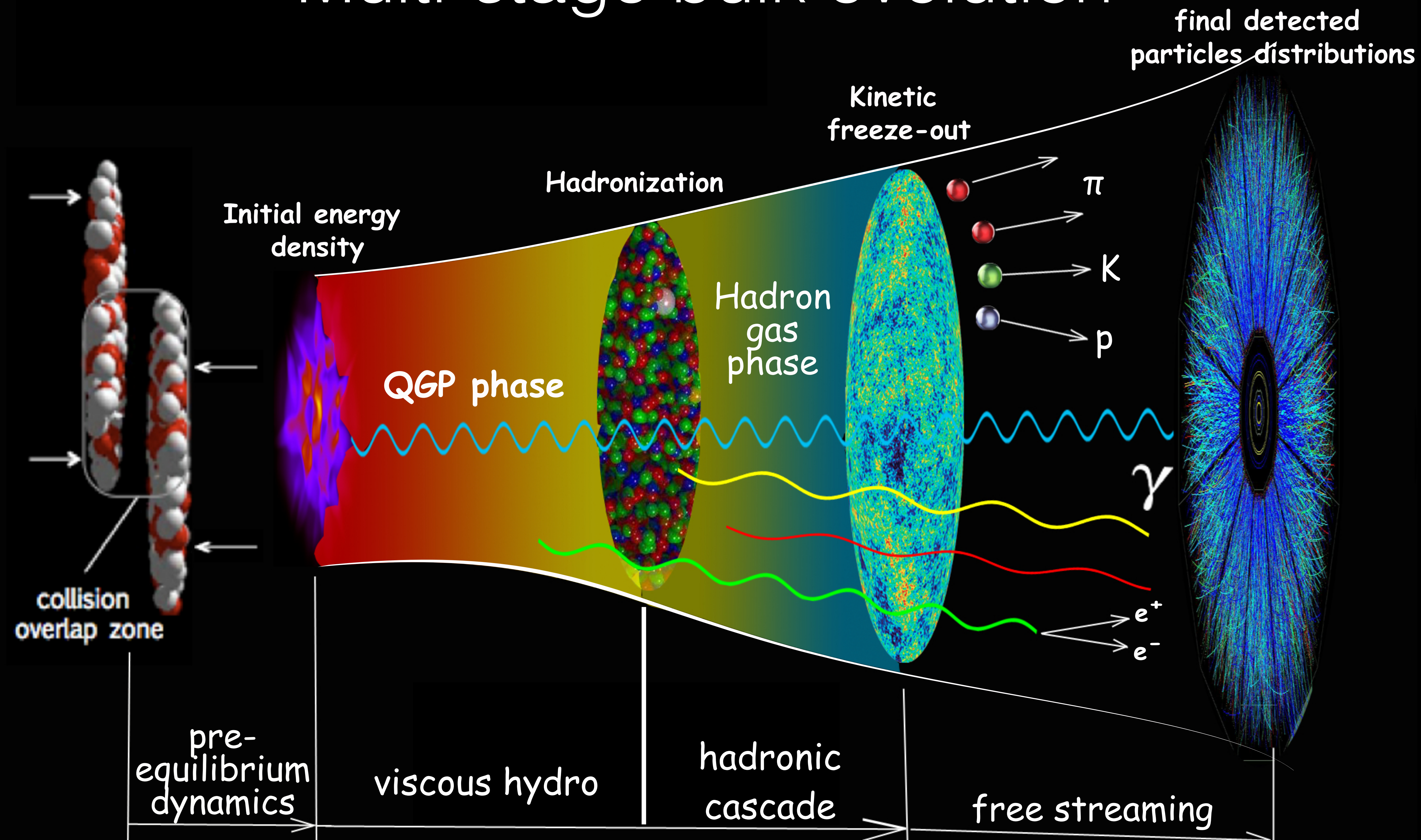

Request for a hybrid framework for RHIC BES

Heavy-ion collisions at RHIC BES

I. A. Karpenko, P. Huovinen, H. Petersen and M. Bleicher, Phys. Rev. C91 (2015) 064901
C. Shen and B. Schenke, Phys. Rev. C97 (2018) 024907

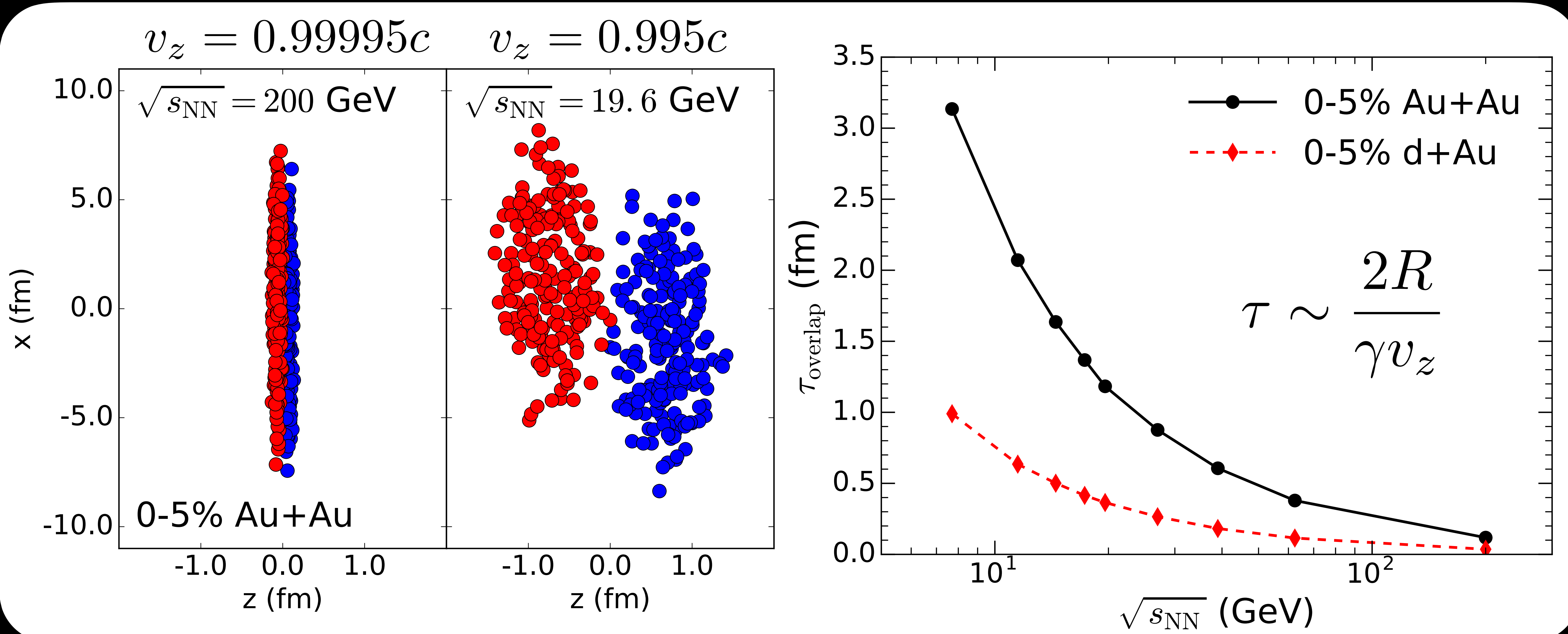

- Nuclei overlapping time is large at low collision energy
- Pre-equilibrium dynamics can play an important role

note: total evolution time ~ 10 fm

3D dynamics beyond the Bjorken paradigm

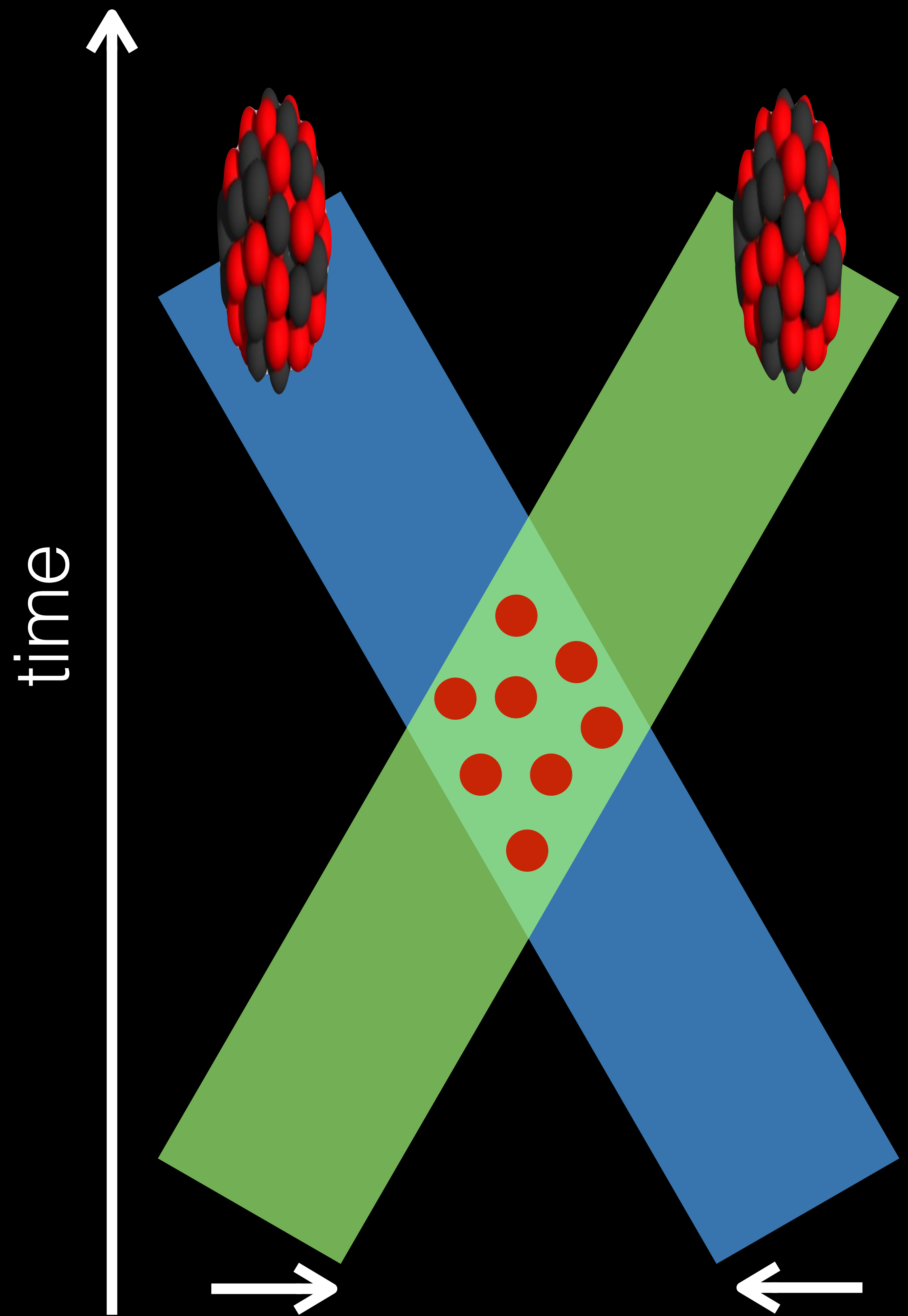

- The interaction zone is not point like
- String based initial condition

  A. Bialas, A. Bzdak and V. Koch, Acta Phys. Polon. B49 (2018)

  C. Shen and B. Schenke, Phys.Rev. C97 (2018) 024907

- Transport model based initial condition

  I. A. Karpenko, P. Huovinen, H. Petersen and M. Bleicher, Phys. Rev. C91 (2015) 064901

  L. Du, U. Heinz and G. Vujanovic, Nucl. Phys. A982 (2019) 407-410

String based initial condition

C. Shen and B. Schenke, Phys.Rev. C97 (2018) 024907

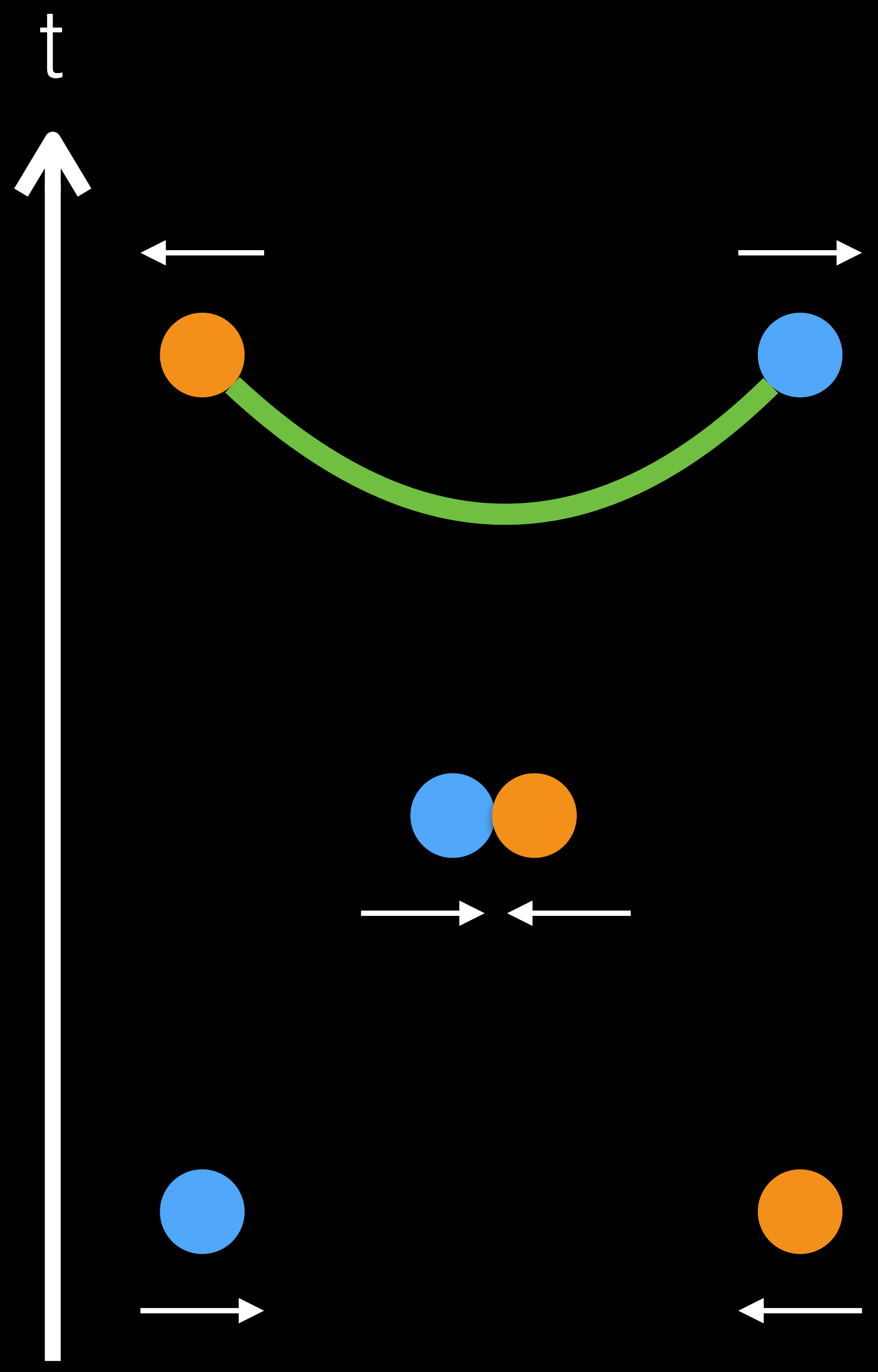

String based initial condition

C. Shen and B. Schenke, Phys.Rev. C97 (2018) 024907

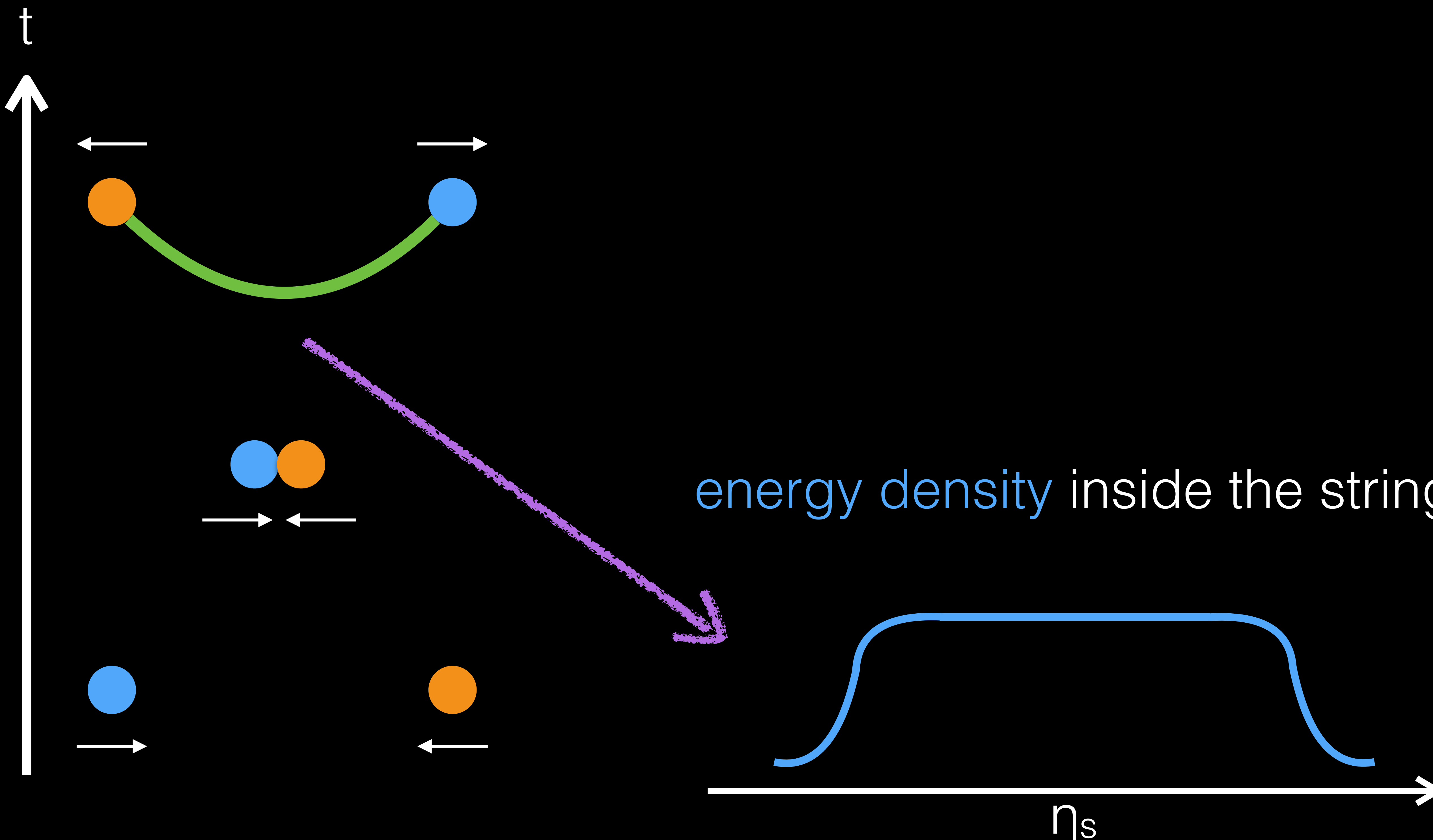

String based initial condition

C. Shen and B. Schenke, Phys.Rev. C97 (2018) 024907

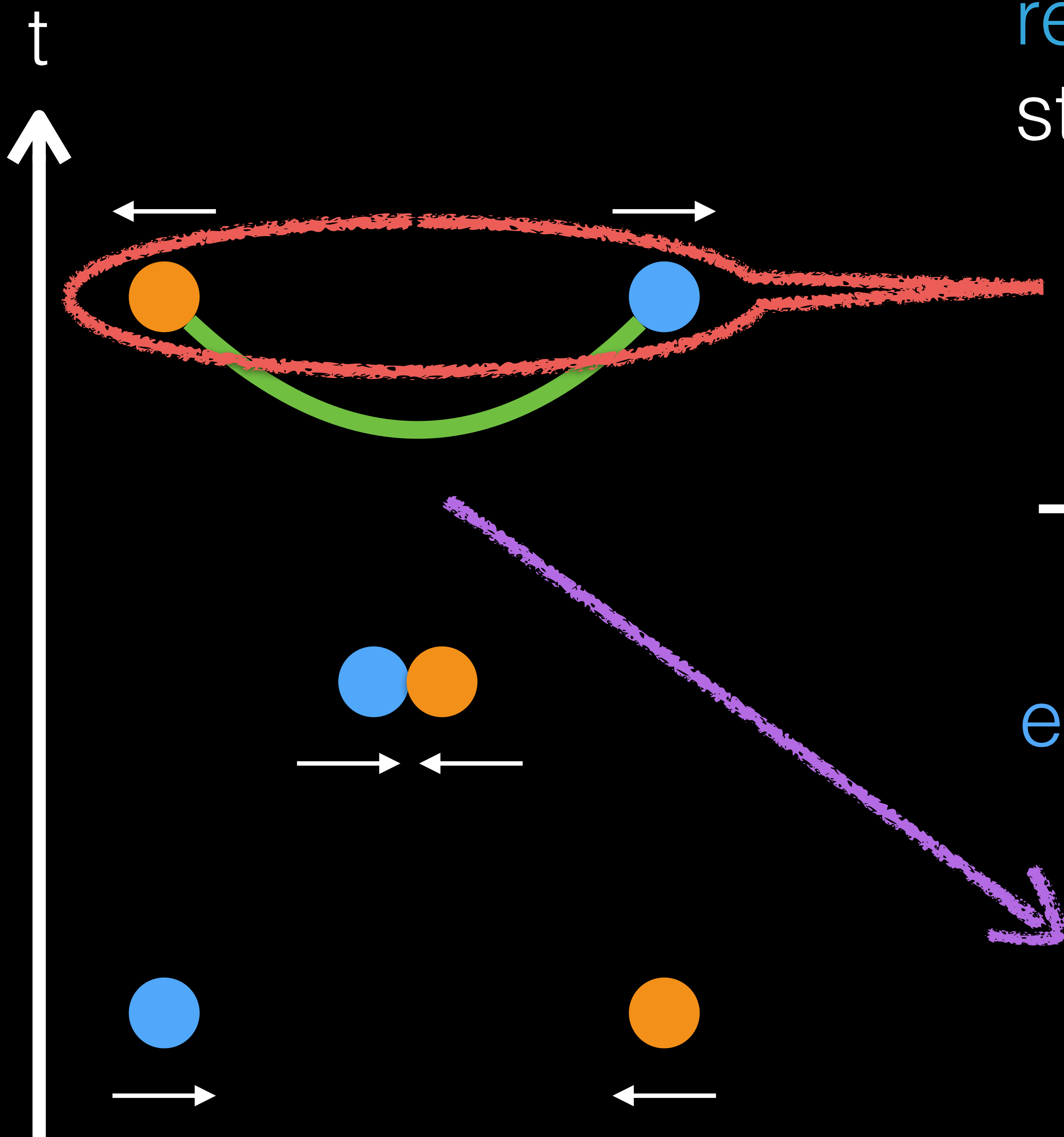

remanent energy density at the string ends

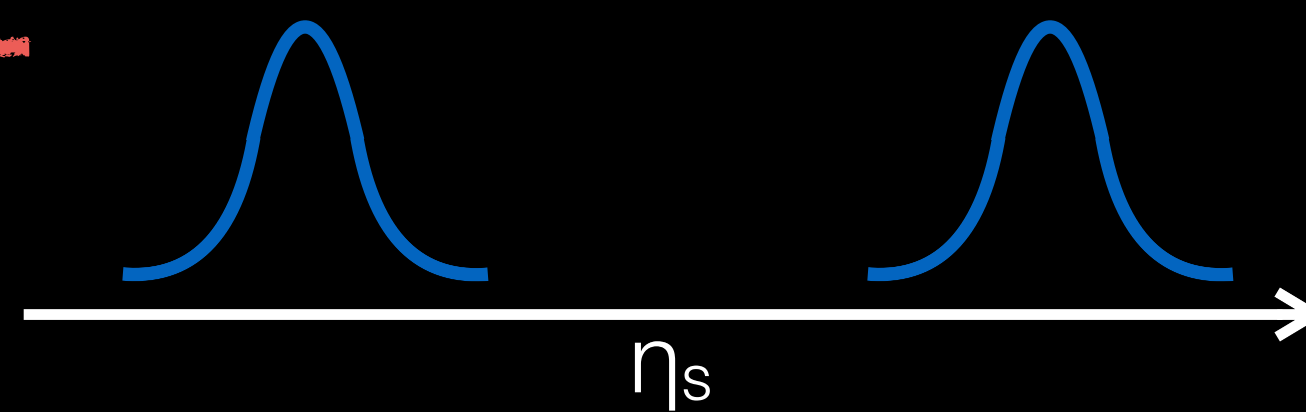

energy density inside the string

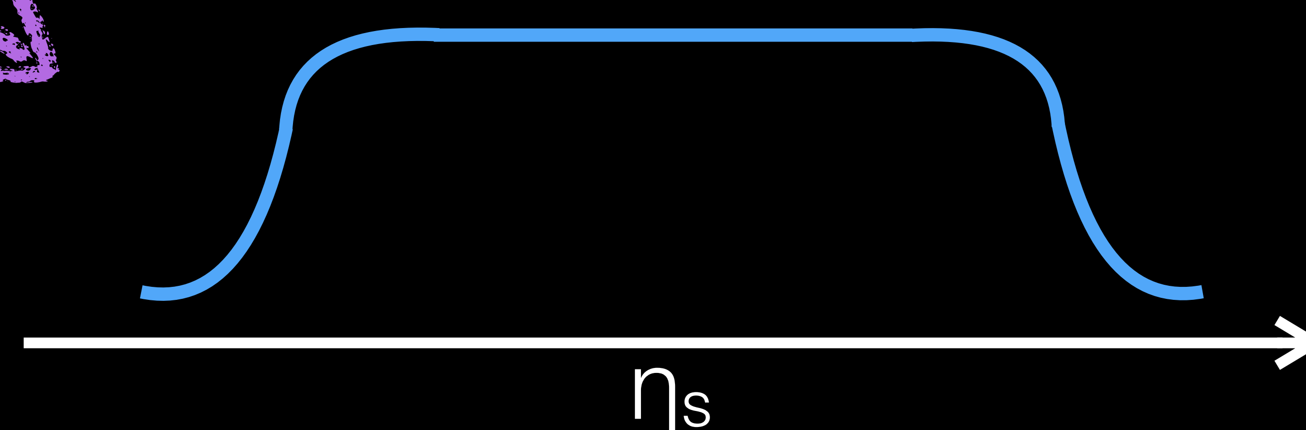

String based initial condition

C. Shen and B. Schenke, Phys.Rev. C97 (2018) 024907

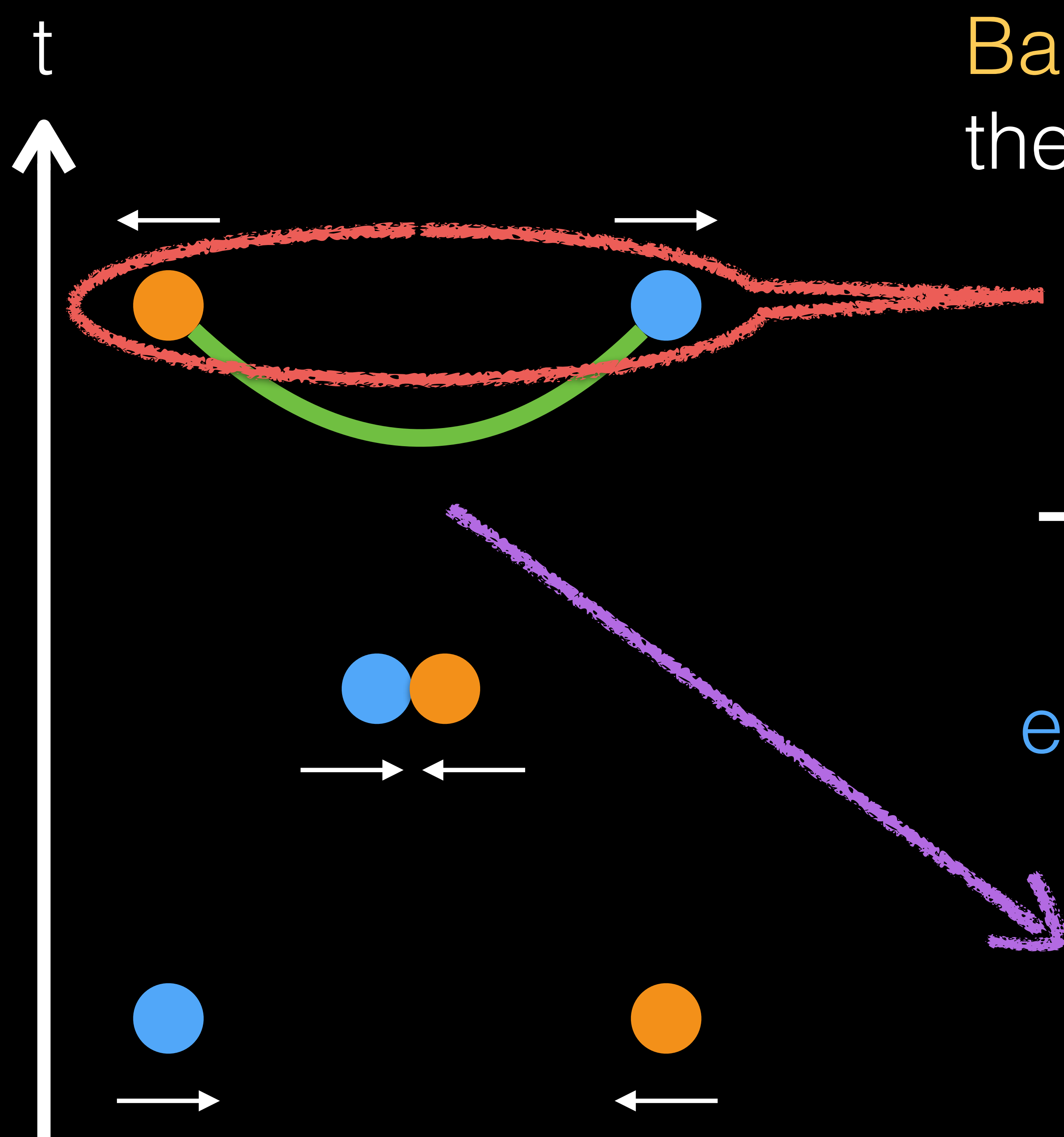

Baryon density are deposited at the string ends

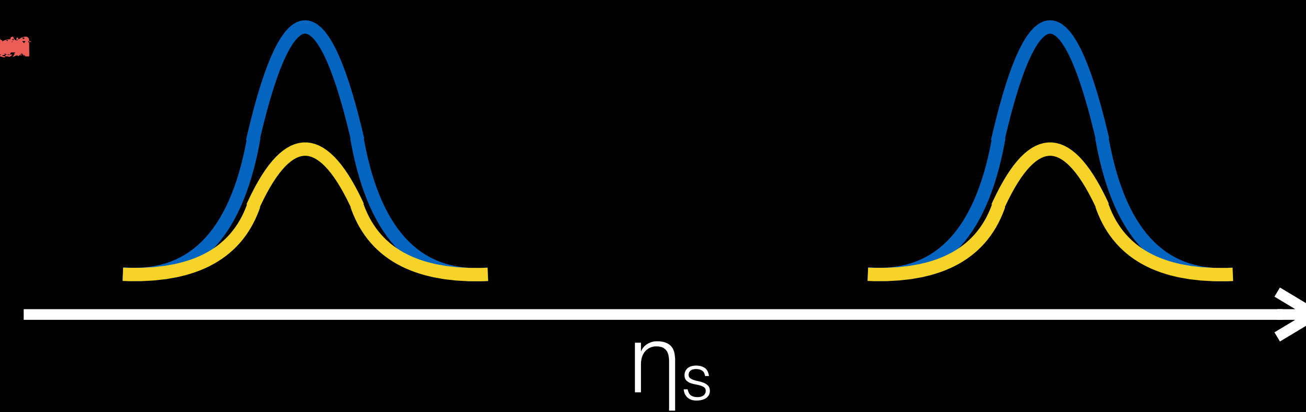

energy density inside the string

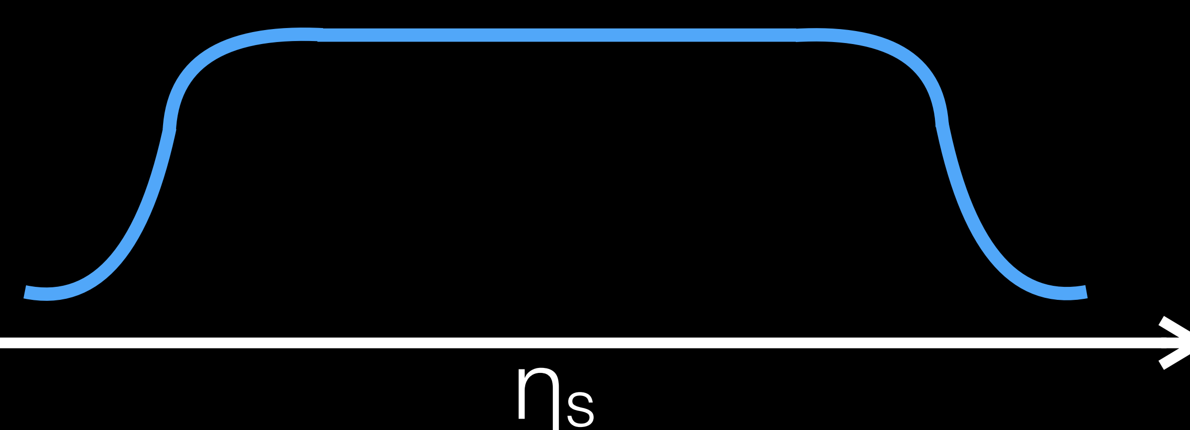

String based initial condition

B. Schenke and C. Shen, in preparation

Baryon density are deposited at the string ends or string junctions

D. Kharzeev, Phys. Lett. B 378, 238 (1996)

energy density inside the string

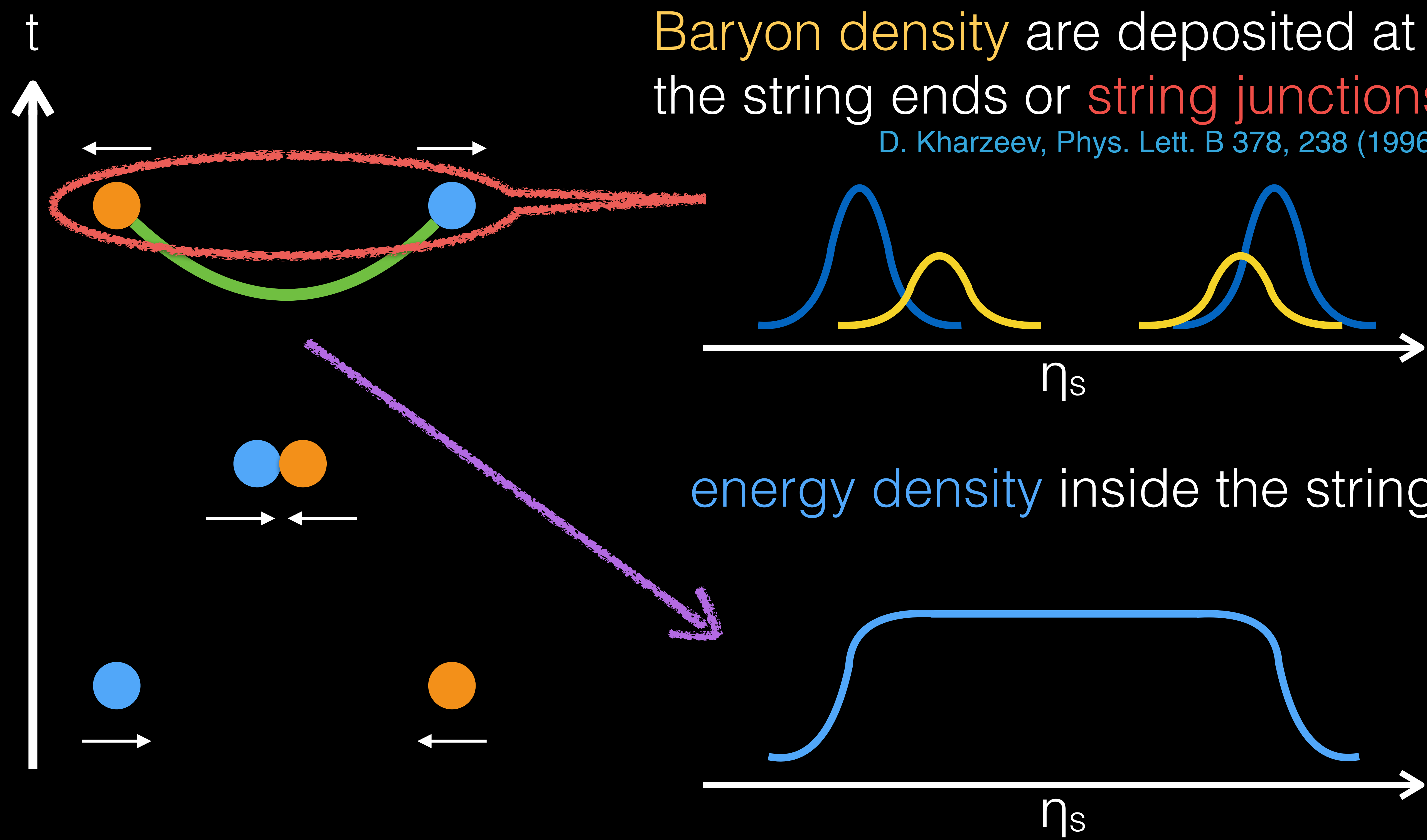

String space-time distribution

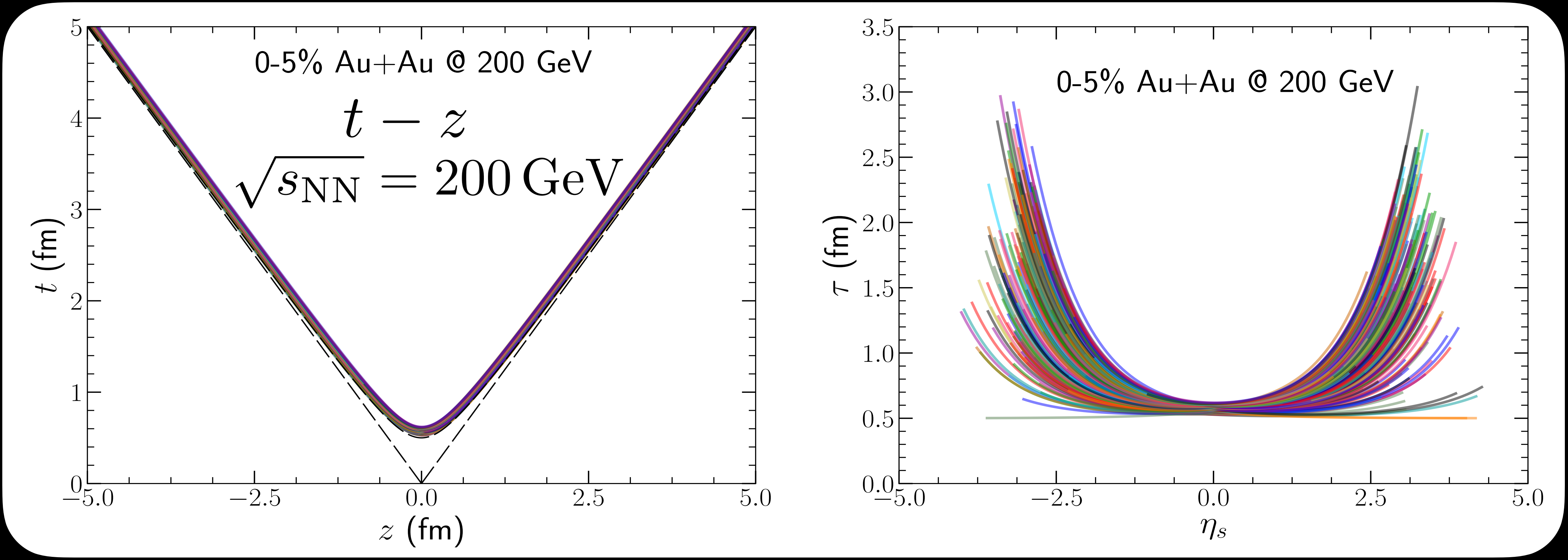

String space-time distribution

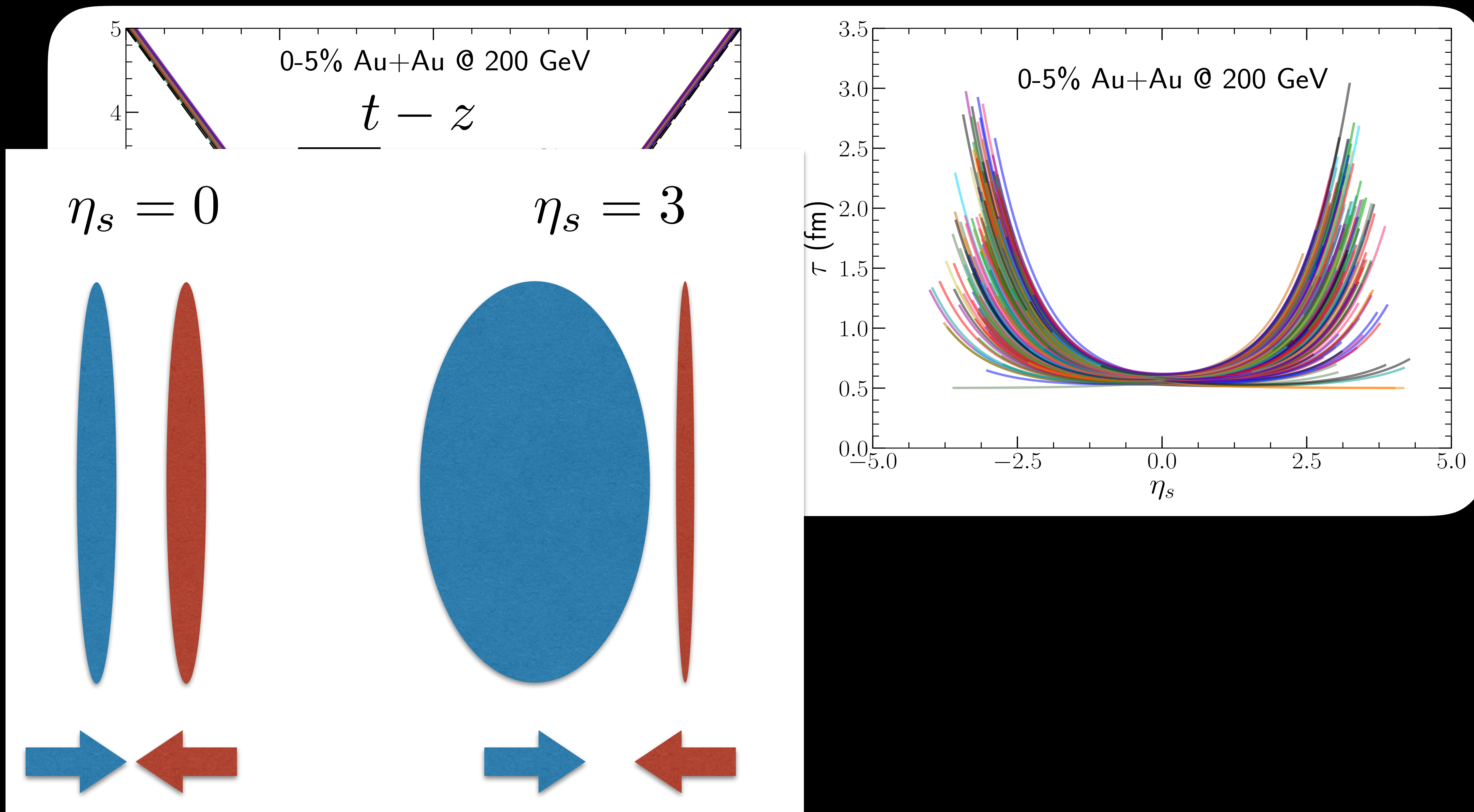

String space-time distribution

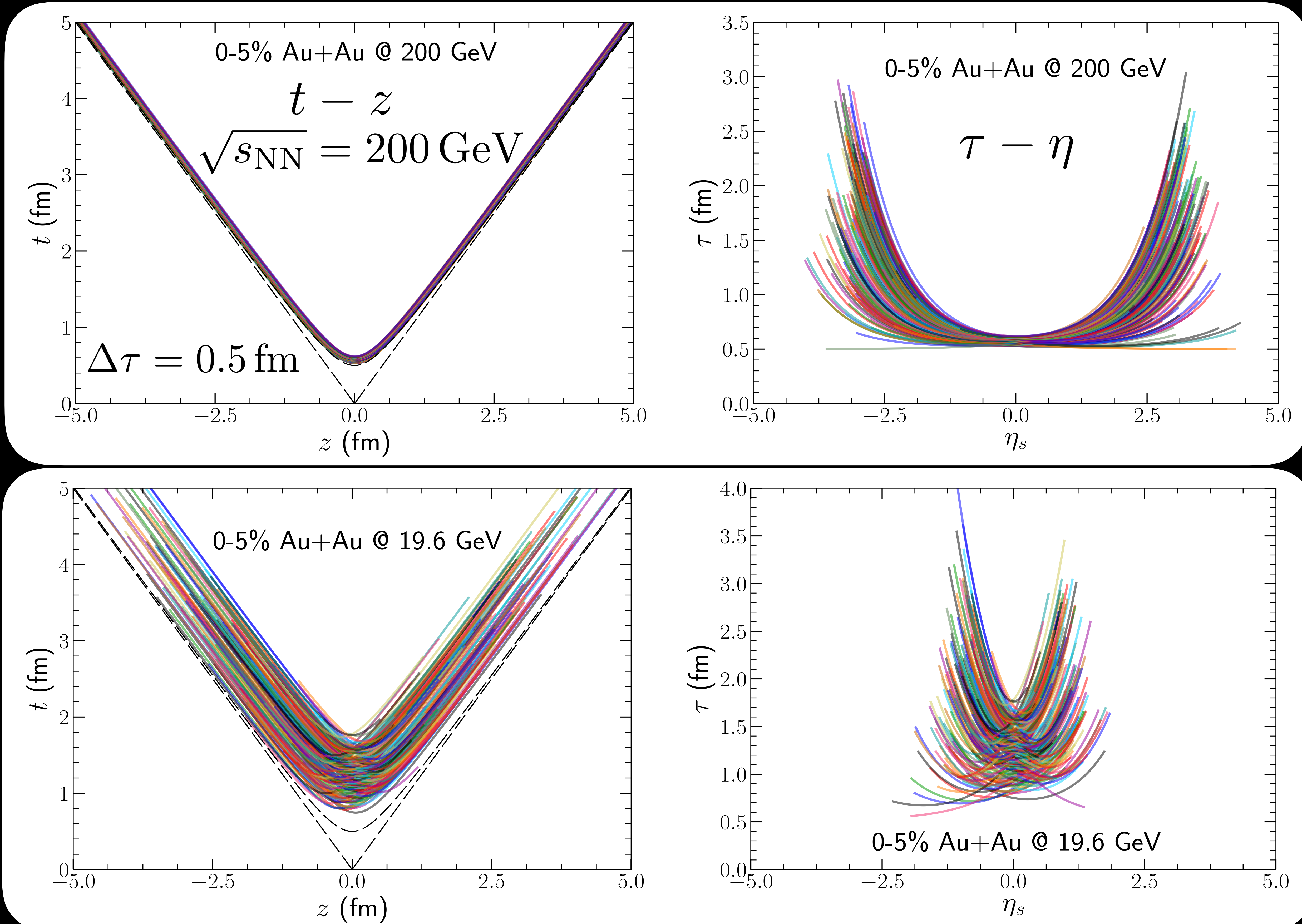

Hydrodynamics with sources

Energy-momentum current and net baryon density are fed into hydrodynamic simulation as source terms

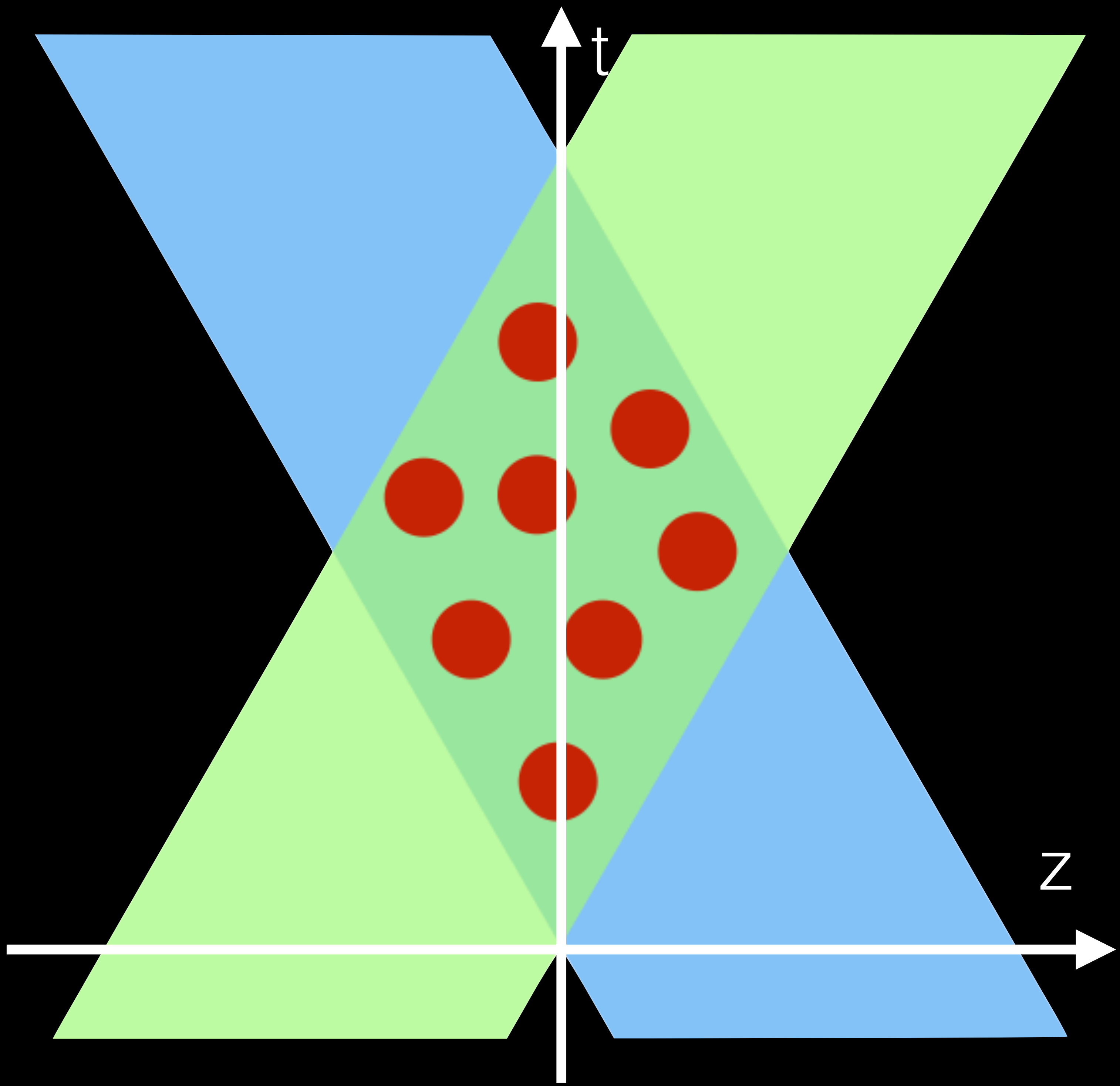

$$\partial_\mu T^{\mu\nu} = J^\nu_{\mathrm{source}}$$
$$\partial_\mu J^\mu = \rho_{\mathrm{source}}$$

C. Shen and B. Schenke,
Phys. Rev. C97 (2018) 024907

L. Du, U. Heinz and G. Vujanovic,
Nucl. Phys. A982 (2019) 407-410

Hydrodynamical evolution with sources

C. Shen and B. Schenke, Phys. Rev. C97 (2018) 024907

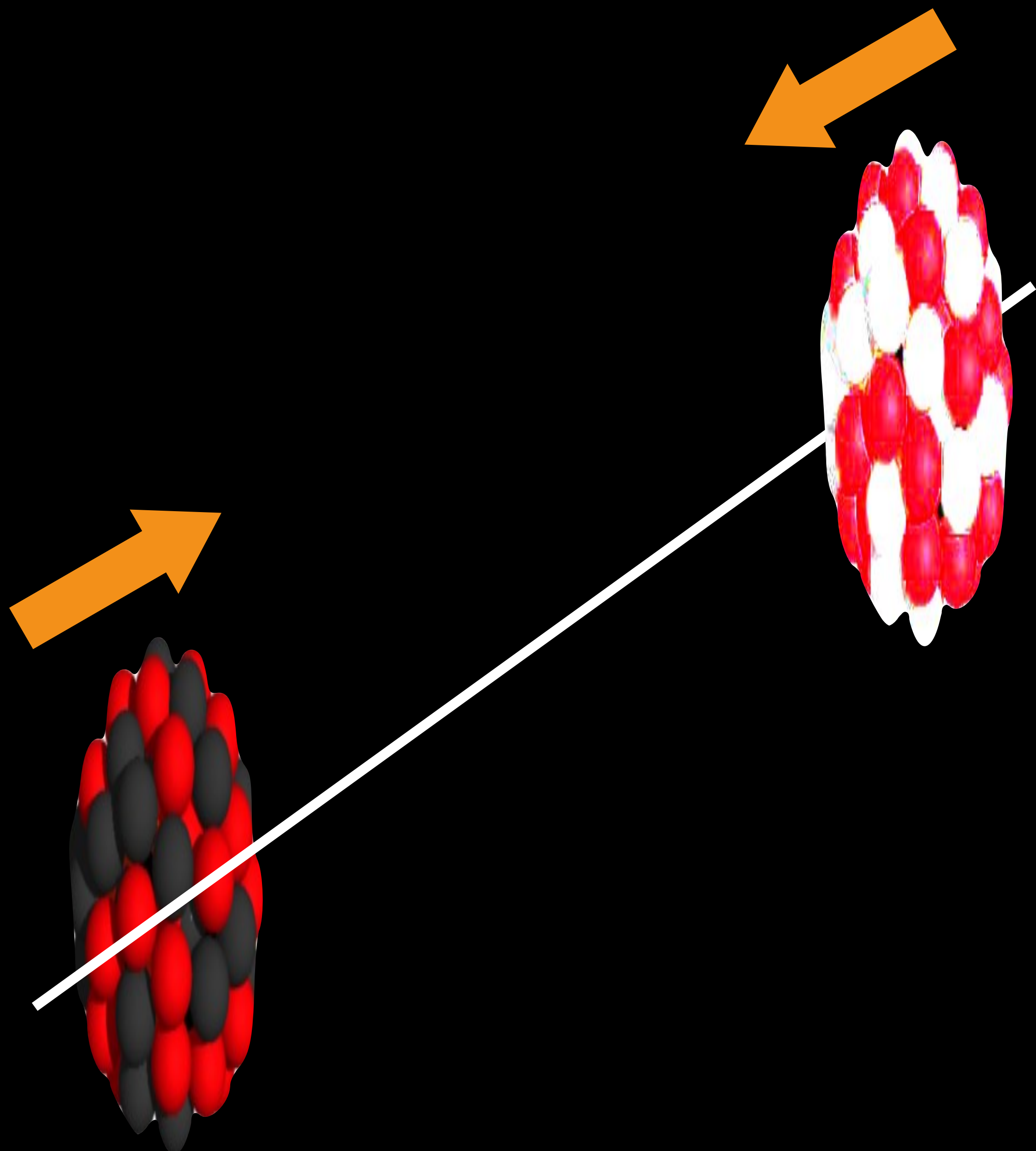

$$\sqrt{s_{\mathrm{NN}}} = 19.6\,\mathrm{GeV}$$

Hydrodynamical evolution with sources

C. Shen and B. Schenke, Phys. Rev. C97 (2018) 024907

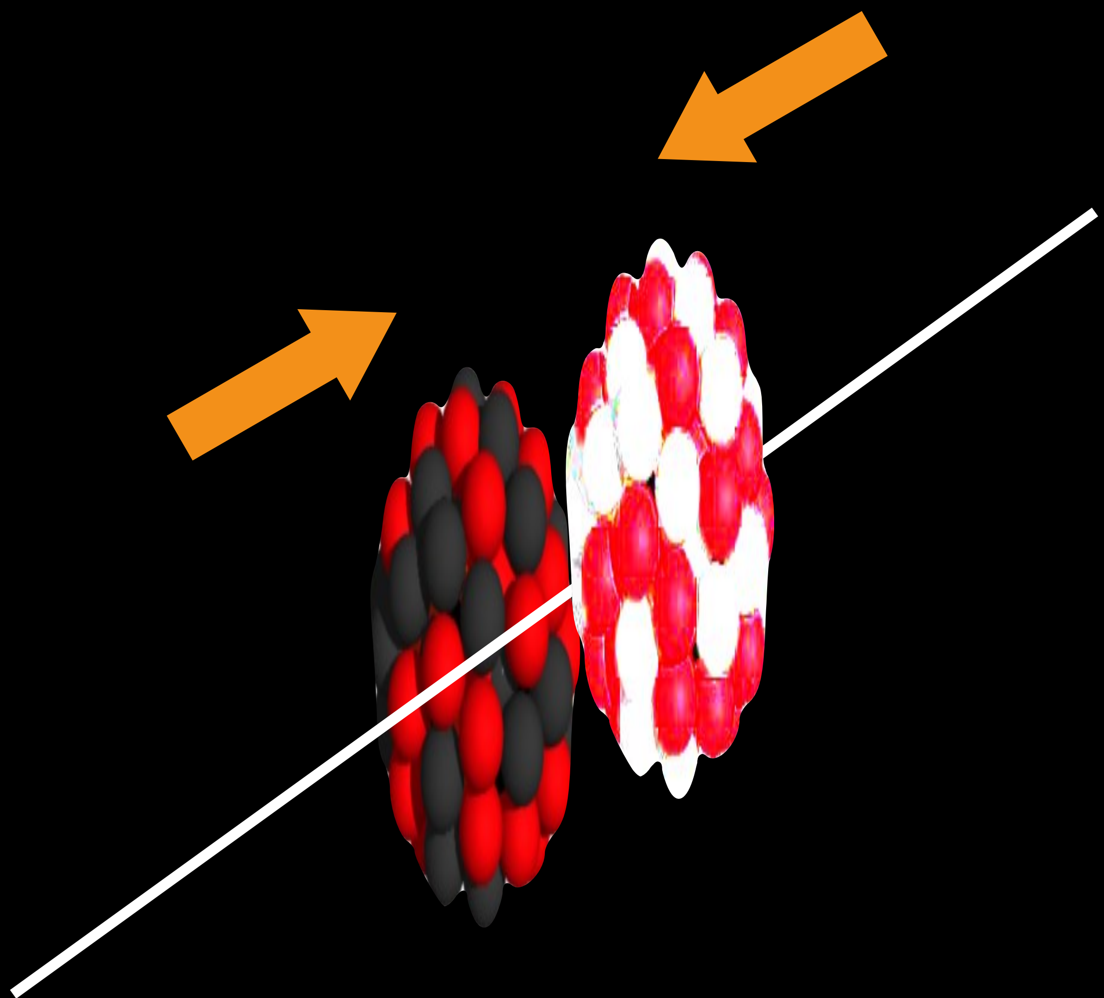

$$\sqrt{s_{\rm NN}} = 19.6\,\mathrm{GeV}$$

Hydrodynamical evolution with sources

C. Shen and B. Schenke, Phys. Rev. C97 (2018) 024907

t=0.5 fm/c

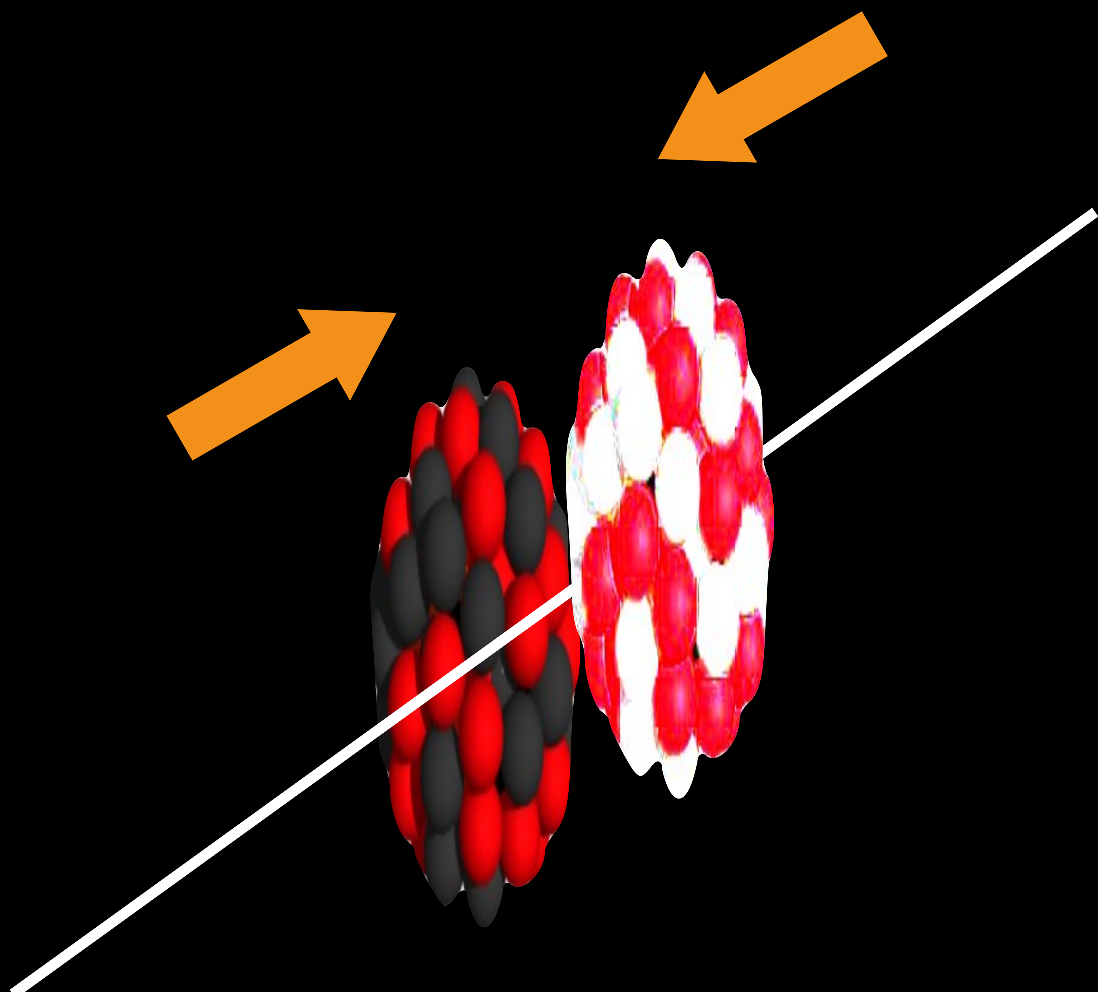

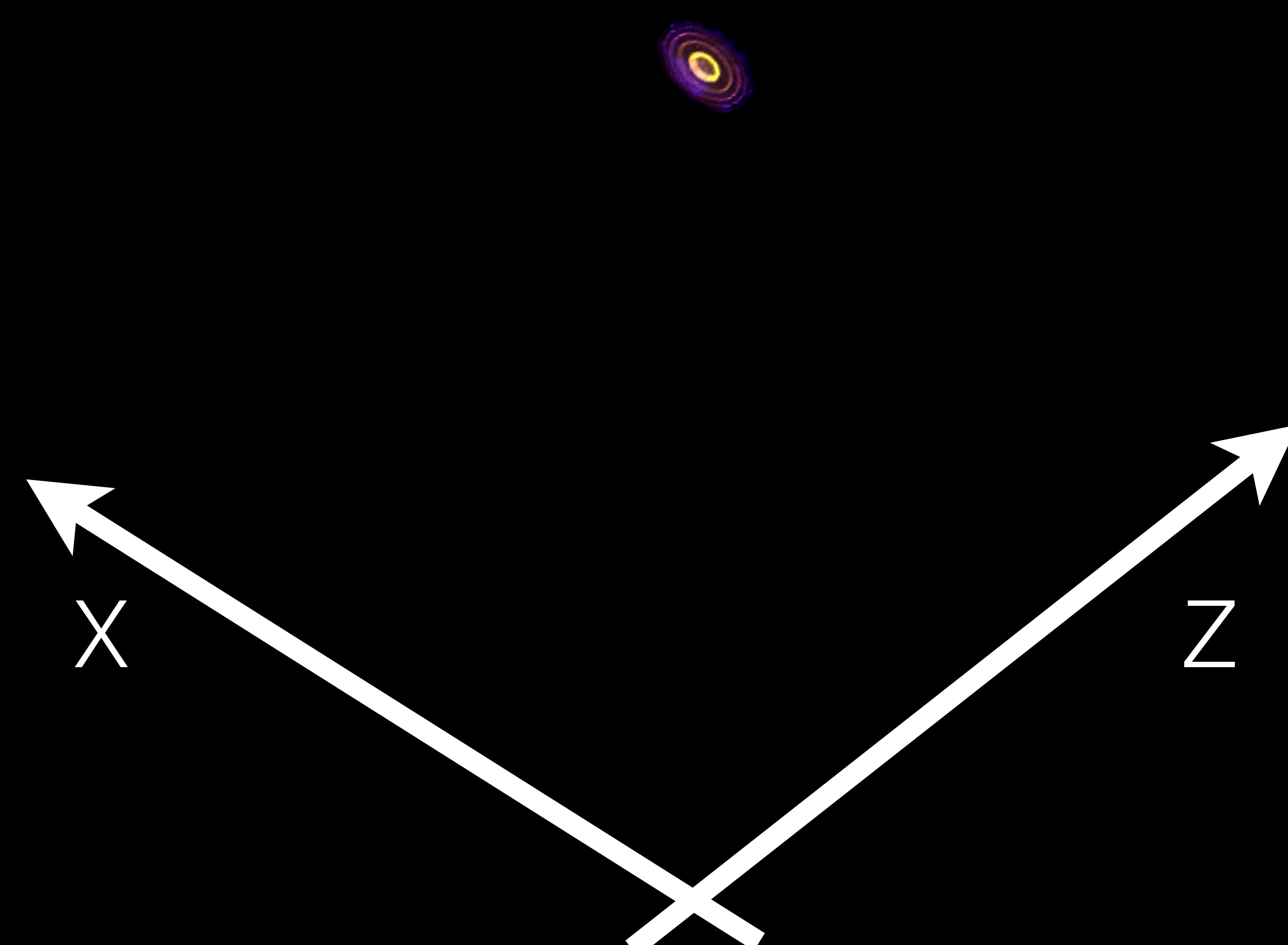

$$\sqrt{s_{\mathrm{NN}}} = 19.6\,\mathrm{GeV}$$

Hydrodynamical evolution with sources

C. Shen and B. Schenke, Phys. Rev. C97 (2018) 024907

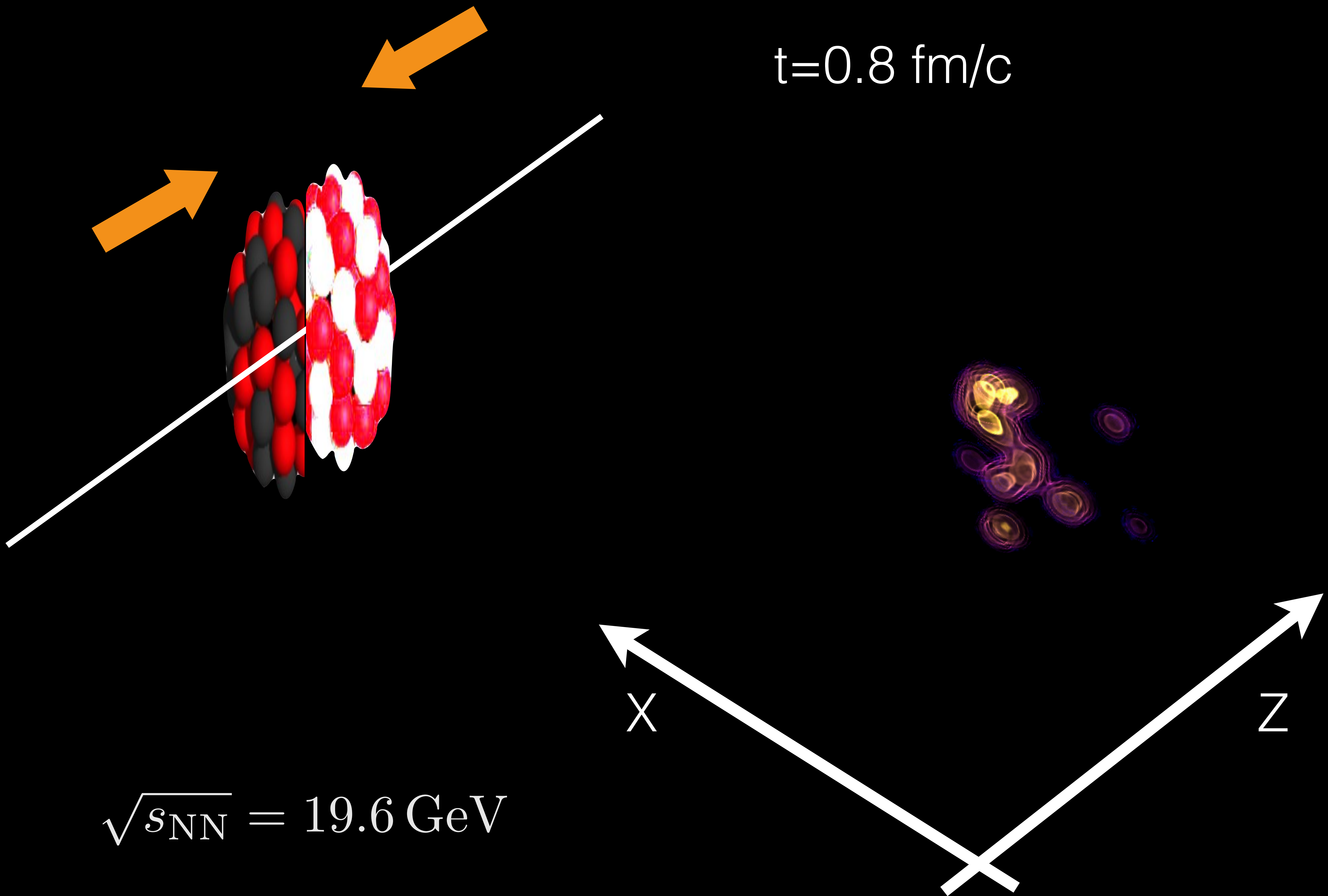

$$\sqrt{s_{\mathrm{NN}}} = 19.6\,\mathrm{GeV}$$

Hydrodynamical evolution with sources

C. Shen and B. Schenke, Phys. Rev. C97 (2018) 024907

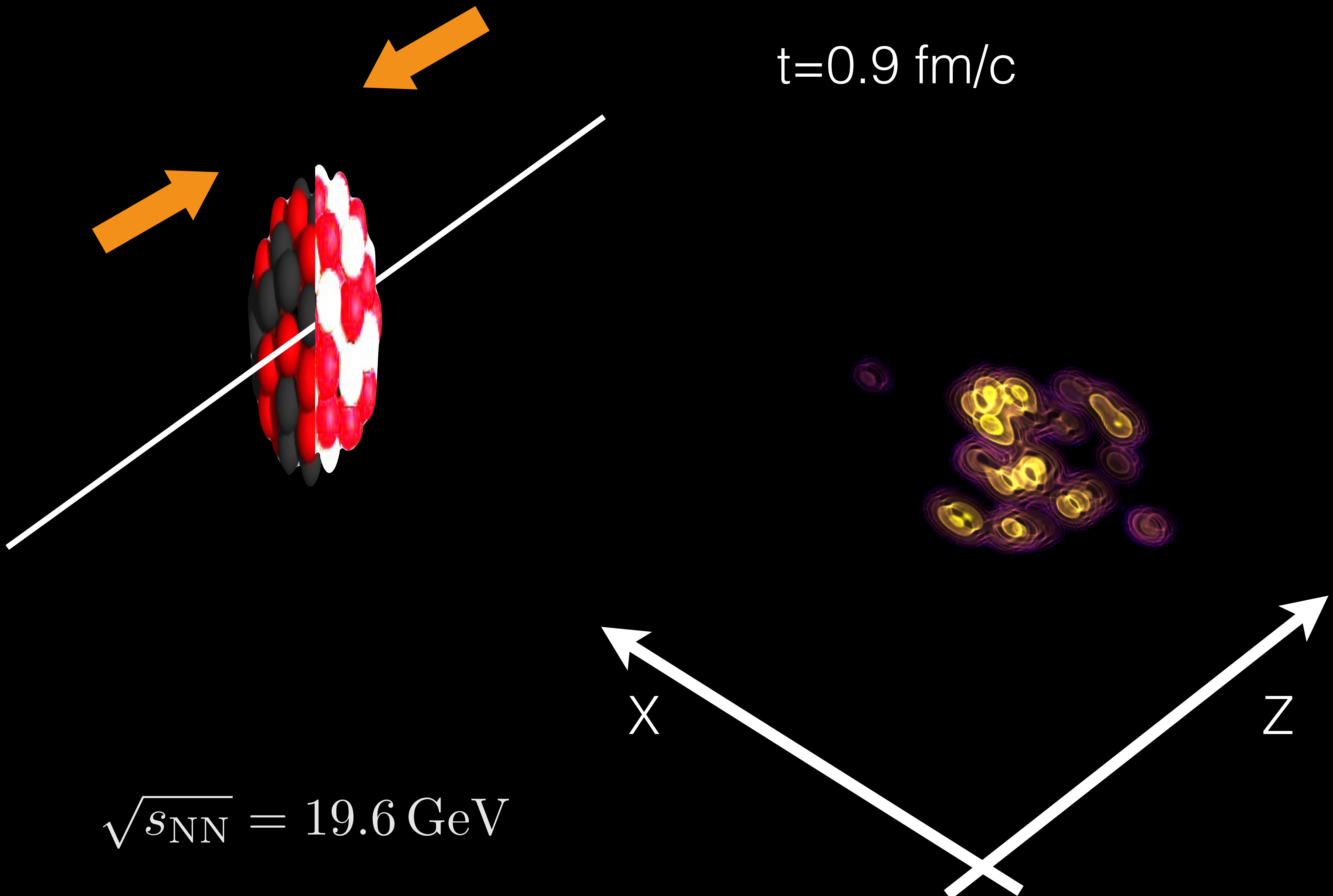

$$\sqrt{s_{\mathrm{NN}}} = 19.6\,\mathrm{GeV}$$

Hydrodynamical evolution with sources

C. Shen and B. Schenke, Phys. Rev. C97 (2018) 024907

t=1.0 fm/c

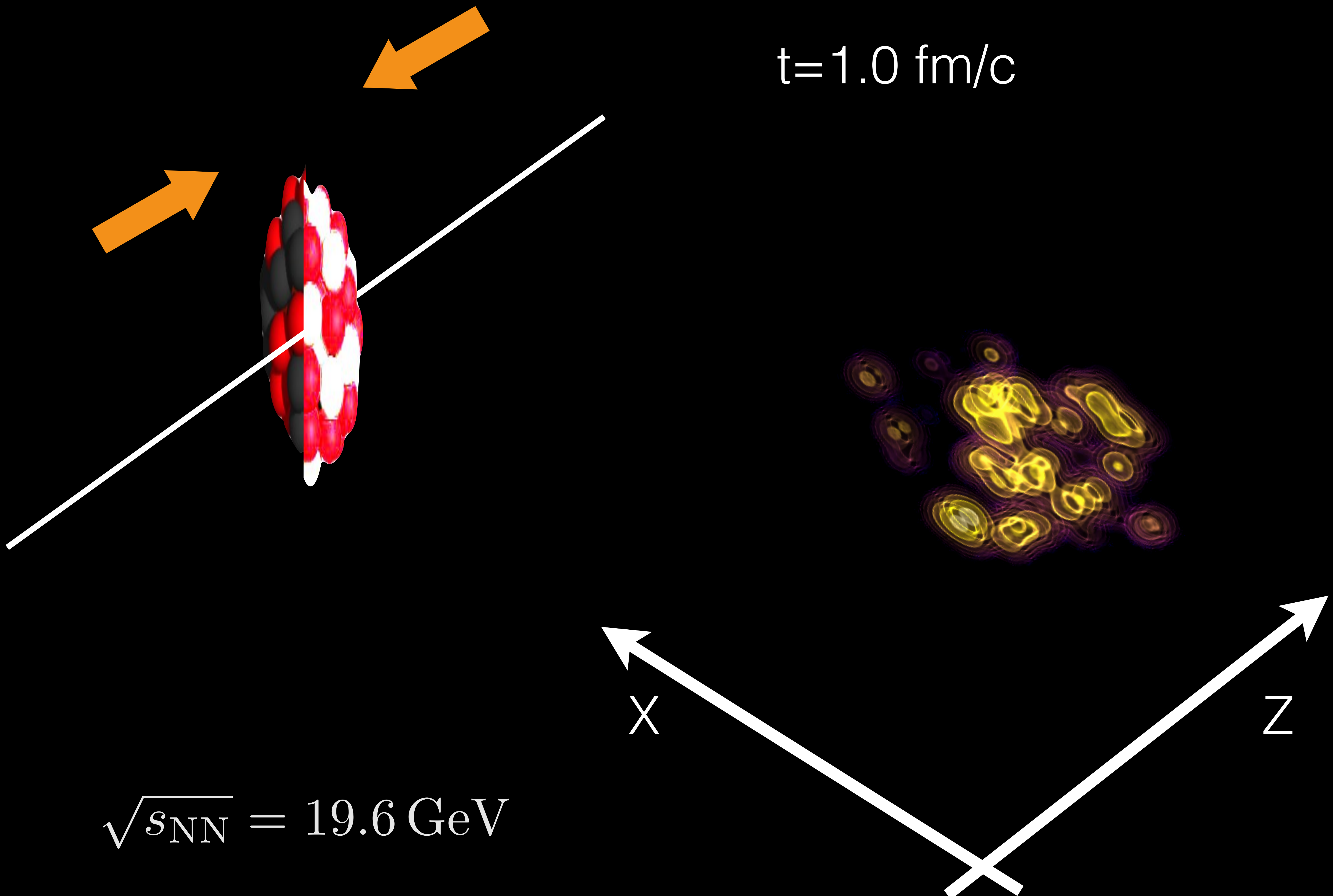

$$\sqrt{s_{\mathrm{NN}}} = 19.6\,\mathrm{GeV}$$

Hydrodynamical evolution with sources

C. Shen and B. Schenke, Phys. Rev. C97 (2018) 024907

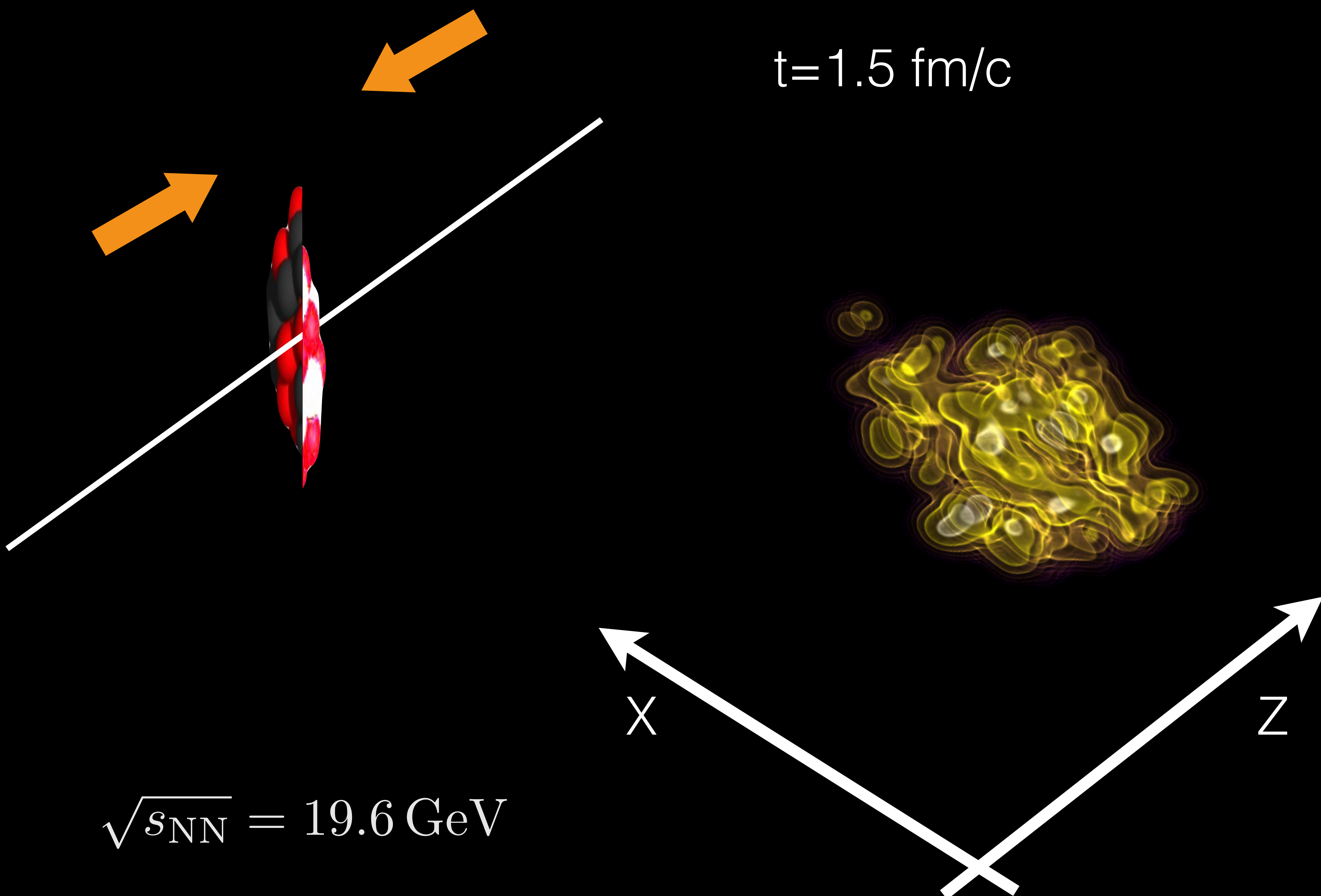

$$\sqrt{s_{\mathrm{NN}}} = 19.6\,\mathrm{GeV}$$

Hydrodynamical evolution with sources

C. Shen and B. Schenke, Phys. Rev. C97 (2018) 024907

t=2.5 fm/c

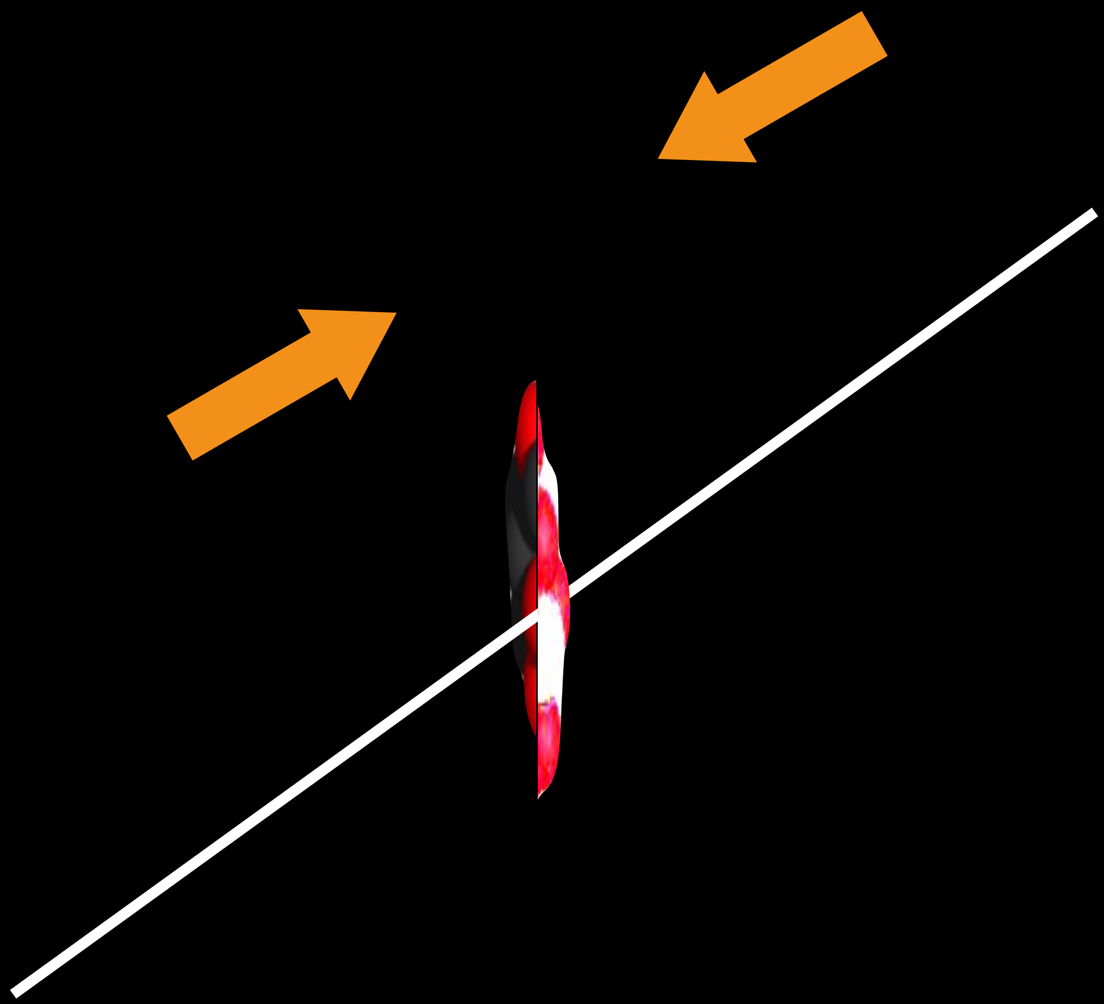

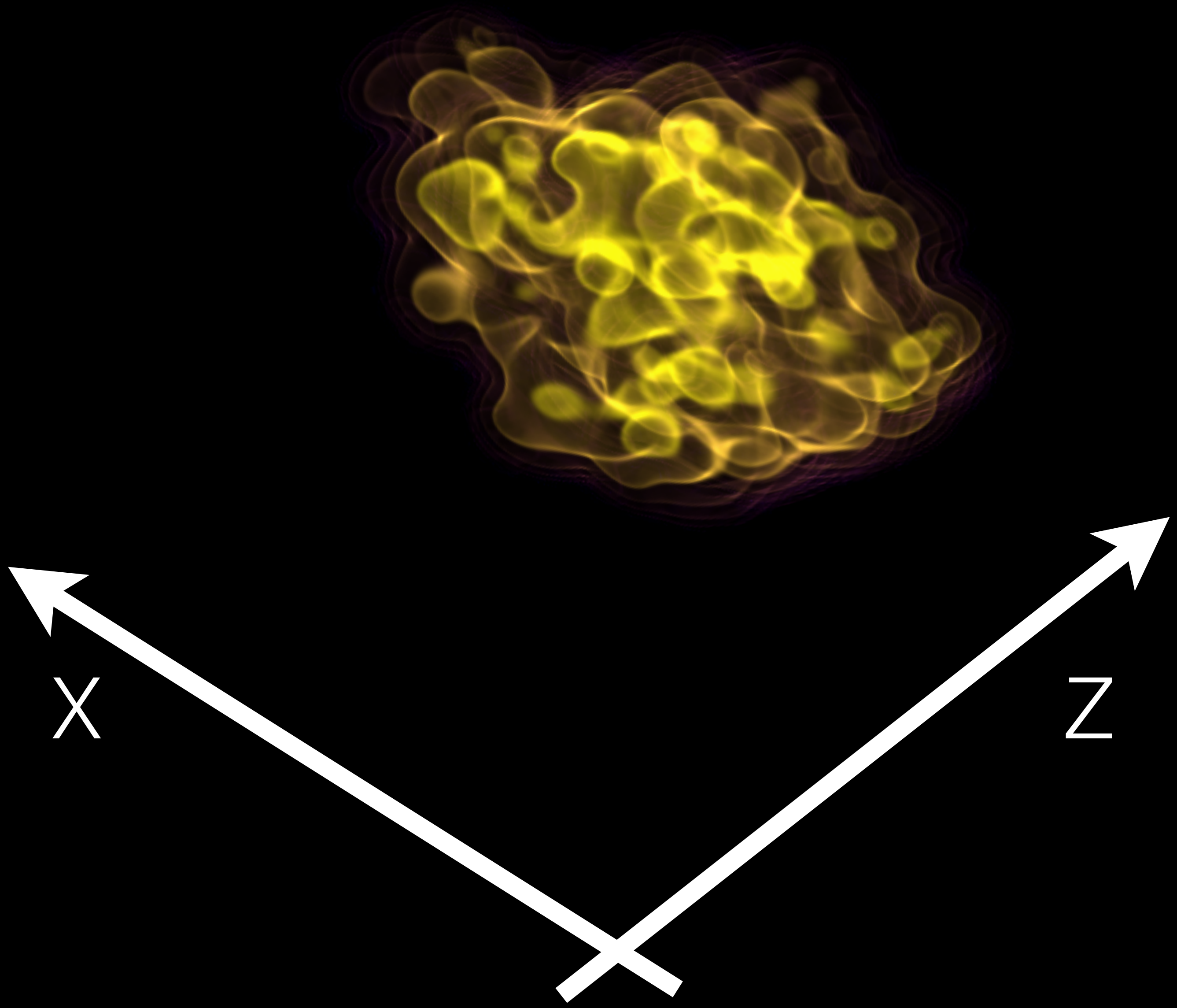

$$\sqrt{s_{\rm NN}} = 19.6\,\mathrm{GeV}$$

Hydrodynamical evolution with sources

C. Shen and B. Schenke, Phys. Rev. C97 (2018) 024907

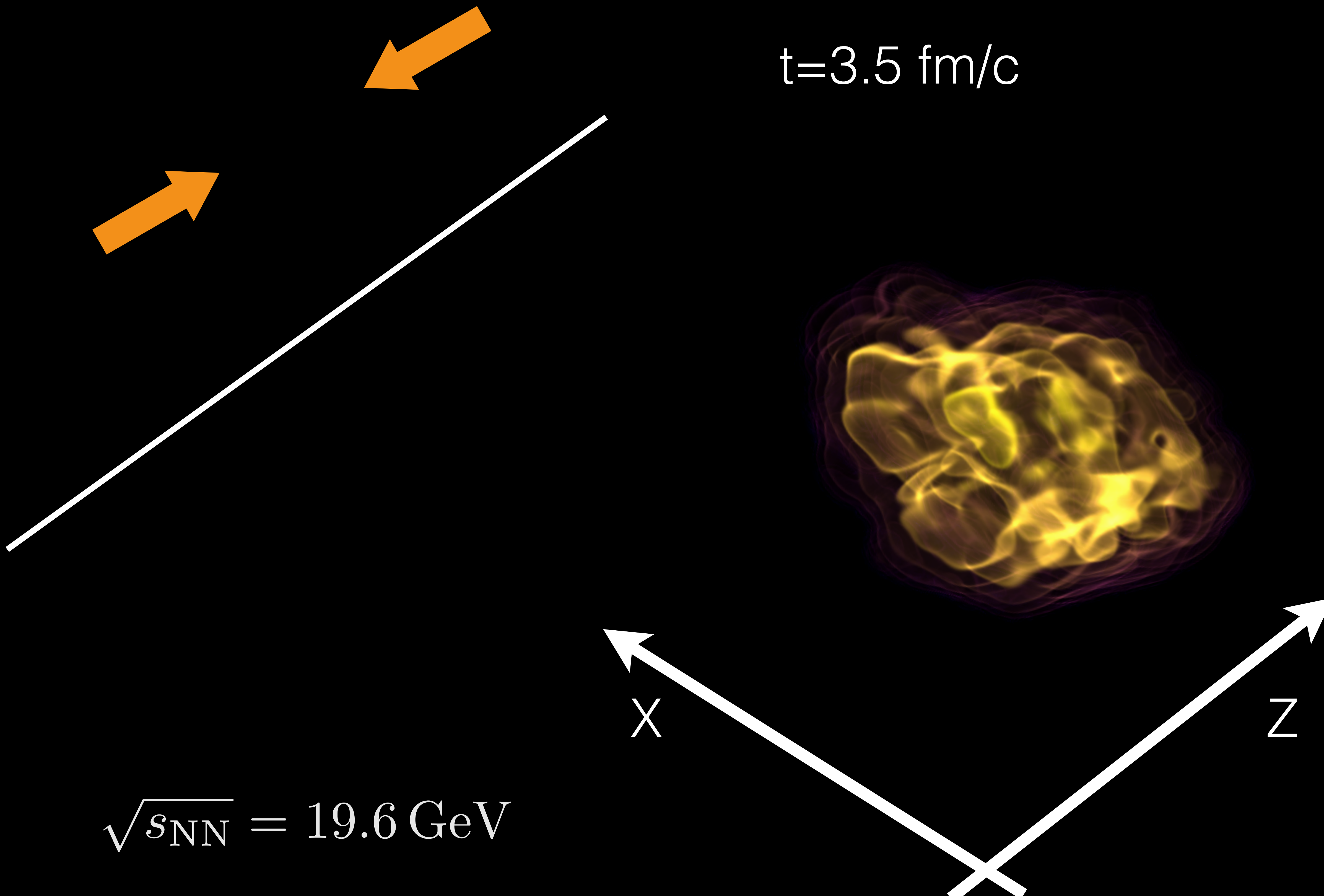

$$\sqrt{s_{\mathrm{NN}}} = 19.6\,\mathrm{GeV}$$

Hydrodynamical evolution with sources

C. Shen and B. Schenke, Phys. Rev. C97 (2018) 024907

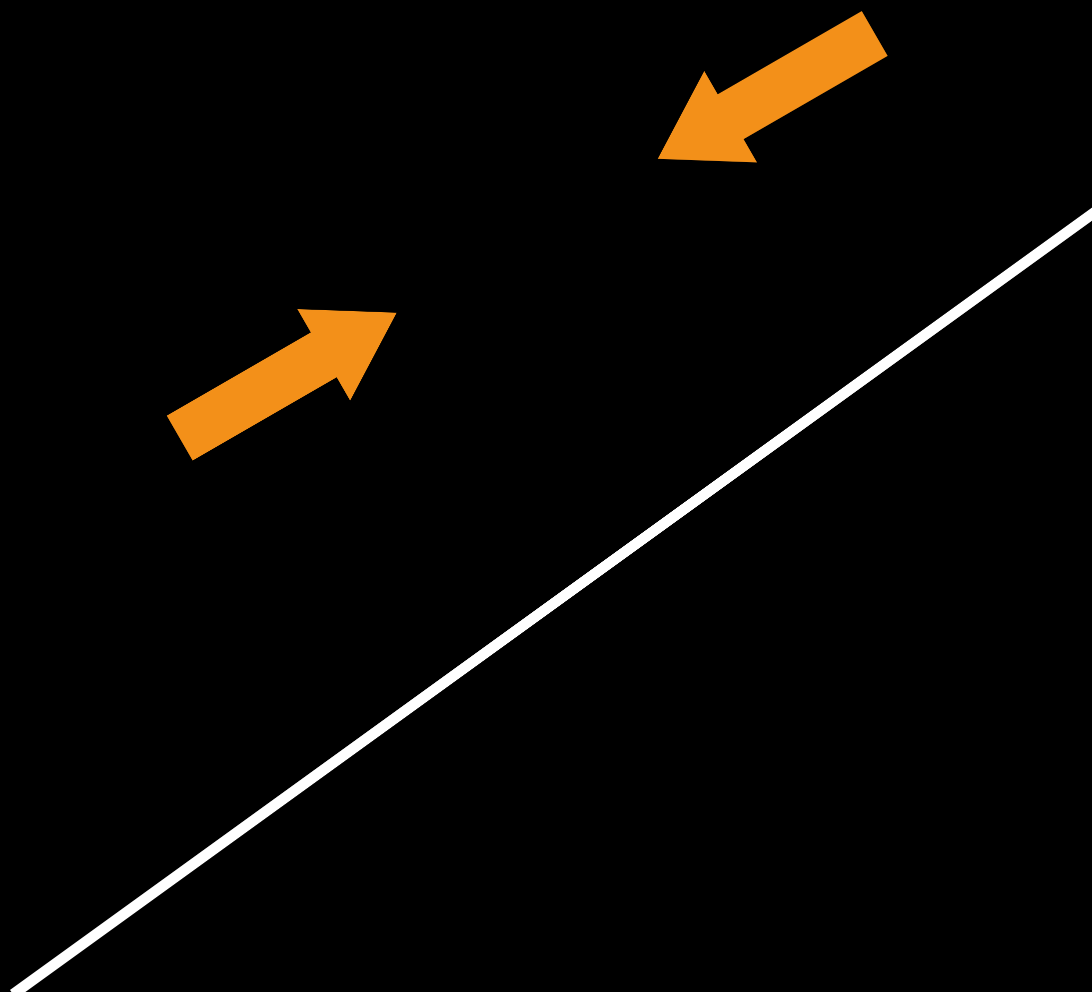

t=5.5 fm/c

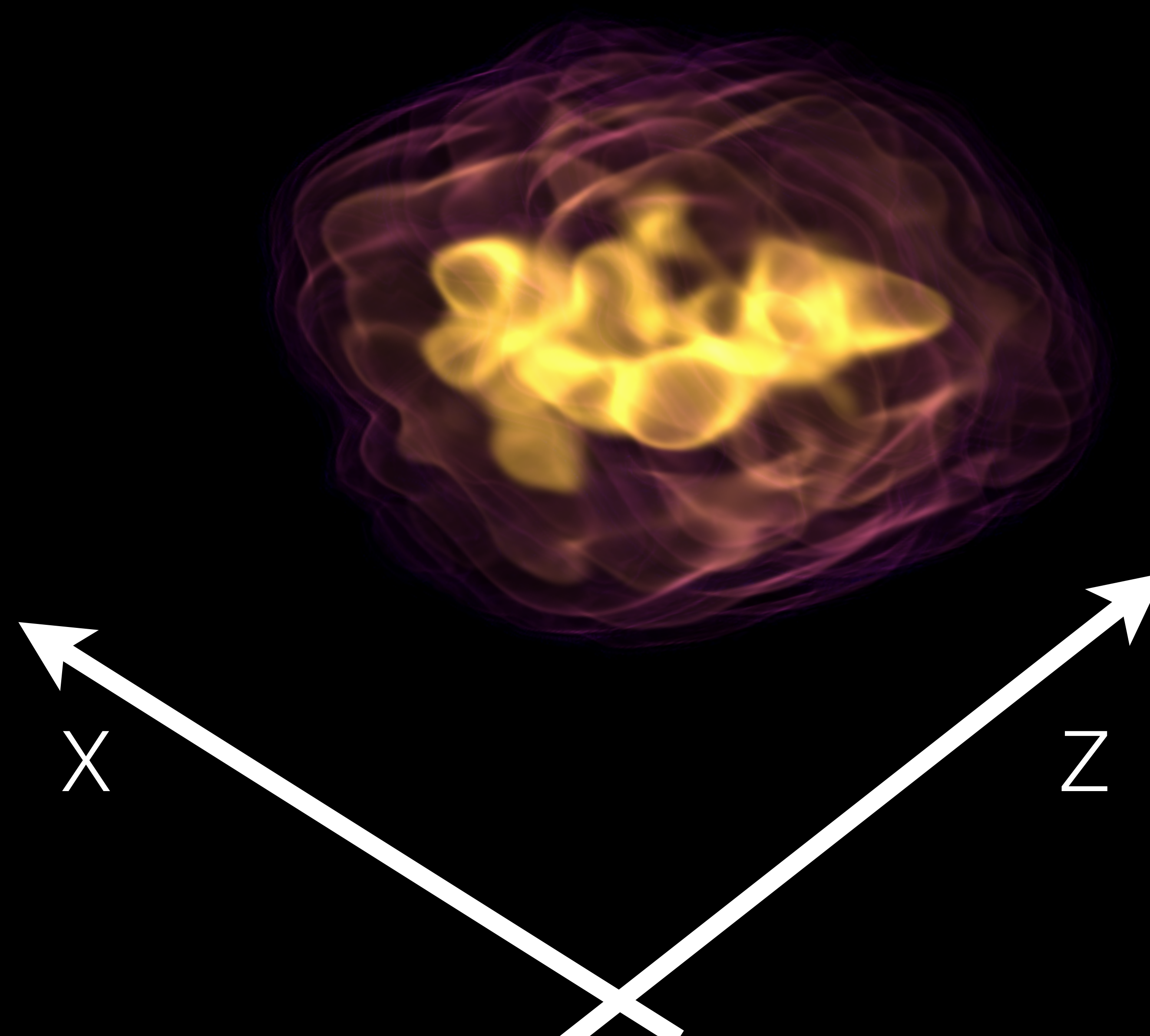

$$\sqrt{s_{\mathrm{NN}}} = 19.6\,\mathrm{GeV}$$

Hydrodynamical evolution with sources

C. Shen and B. Schenke, Phys. Rev. C97 (2018) 024907

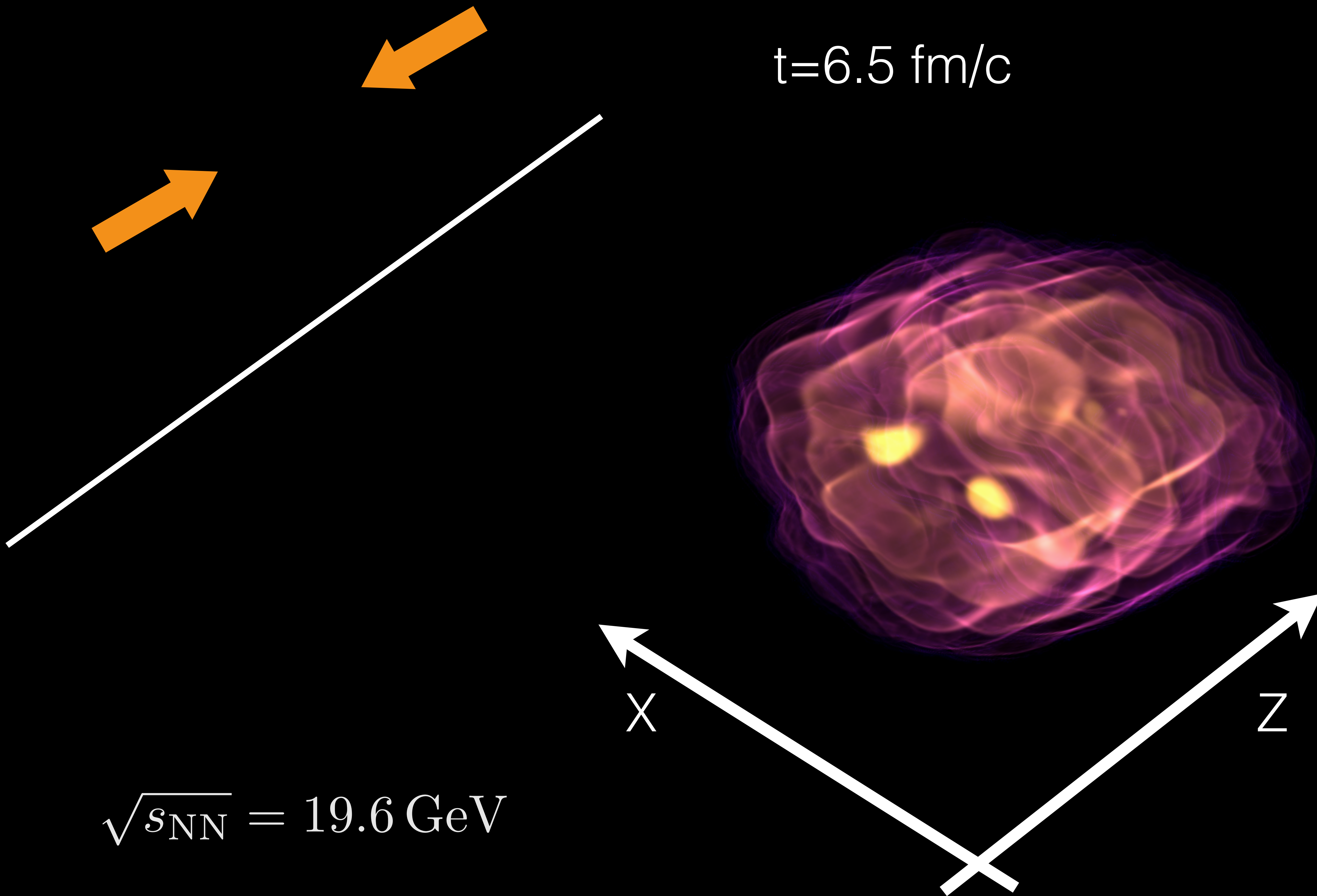

$$\sqrt{s_{\mathrm{NN}}} = 19.6\,\mathrm{GeV}$$

Hydrodynamical evolution with sources

C. Shen and B. Schenke, Phys. Rev. C97 (2018) 024907

t=7.5 fm/c

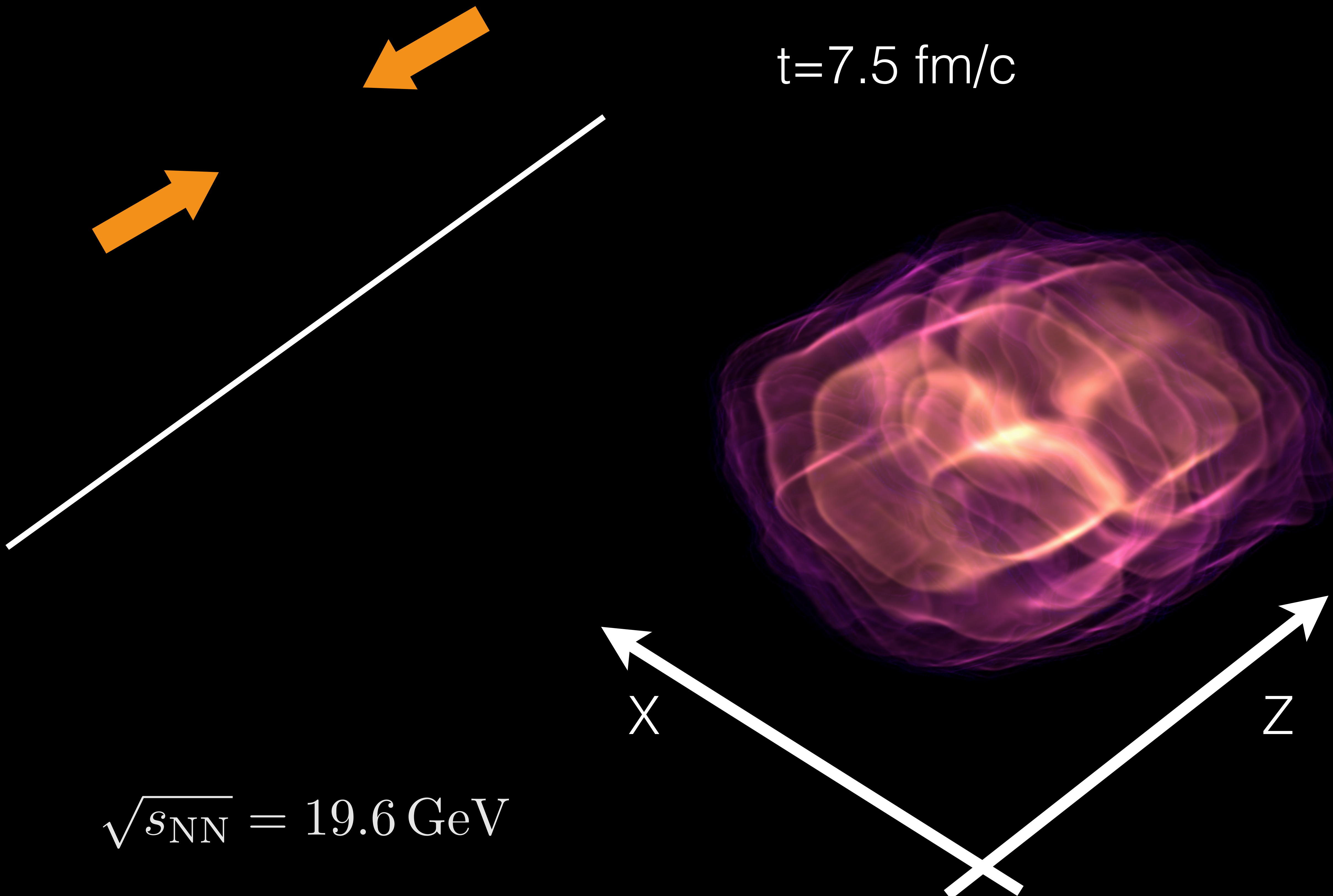

$$\sqrt{s_{\mathrm{NN}}} = 19.6\,\mathrm{GeV}$$

Hydrodynamical evolution with sources

C. Shen and B. Schenke, Phys. Rev. C97 (2018) 024907

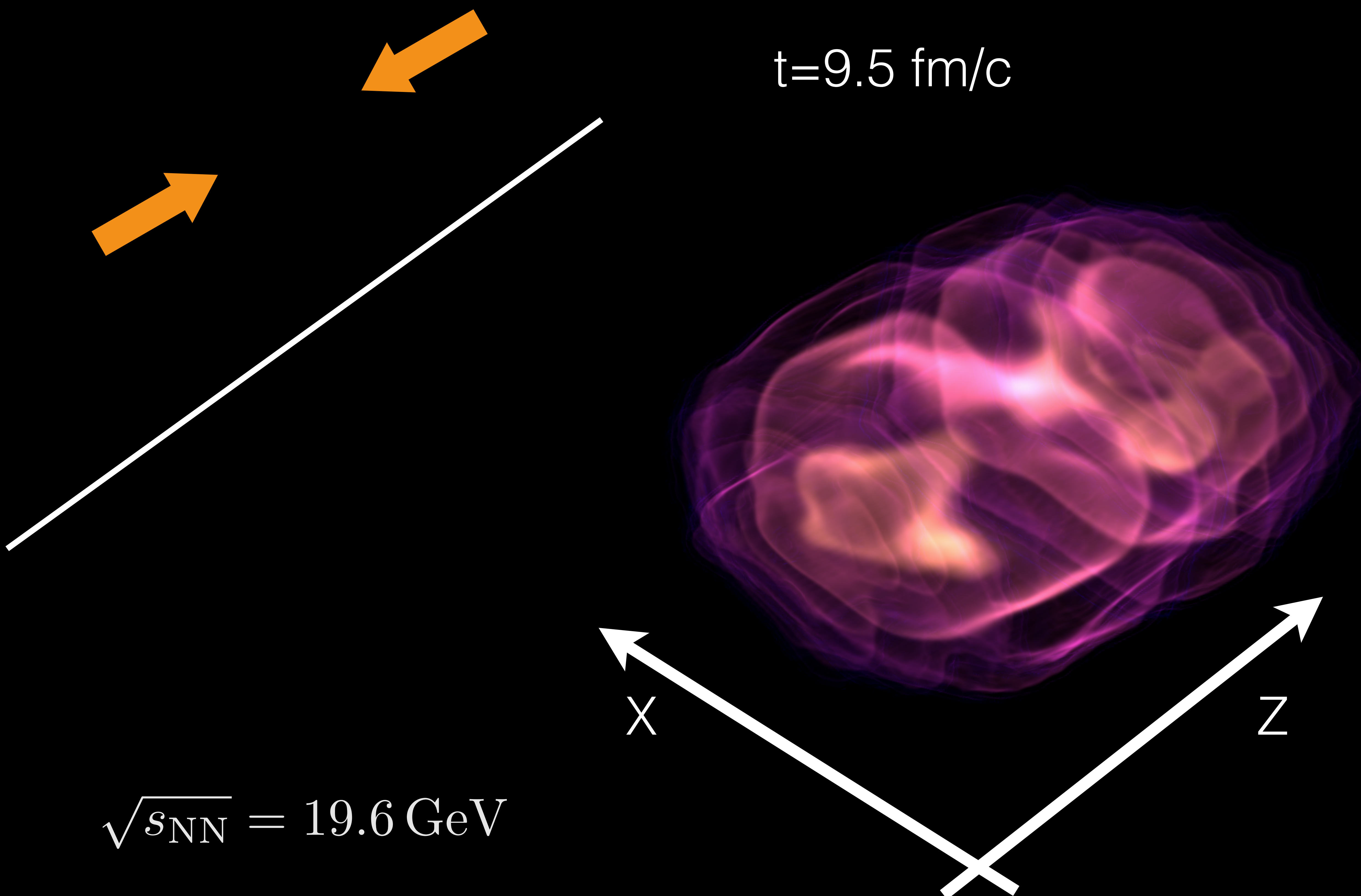

$$\sqrt{s_{\mathrm{NN}}} = 19.6\,\mathrm{GeV}$$

Hydrodynamical evolution with sources

C. Shen and B. Schenke, Phys. Rev. C97 (2018) 024907

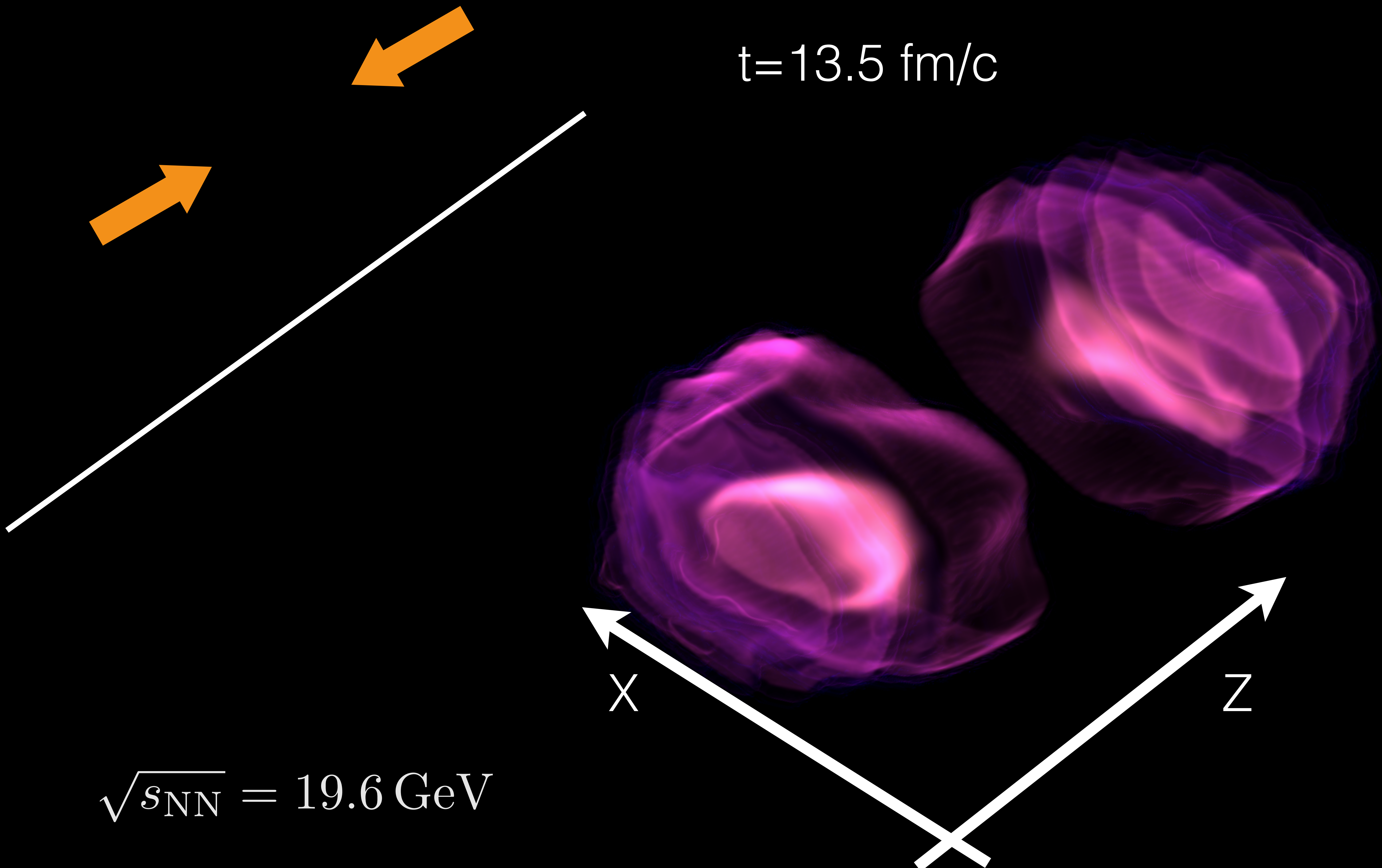

$$\sqrt{s_{\mathrm{NN}}} = 19.6\,\mathrm{GeV}$$

QCD Equation of State at finite densities

A. Monnai, B. Schenke and C. Shen, arXiv:1902.05095 [nucl-th]

$$n_S = 0$$
$$n_Q = 0.4 n_B$$

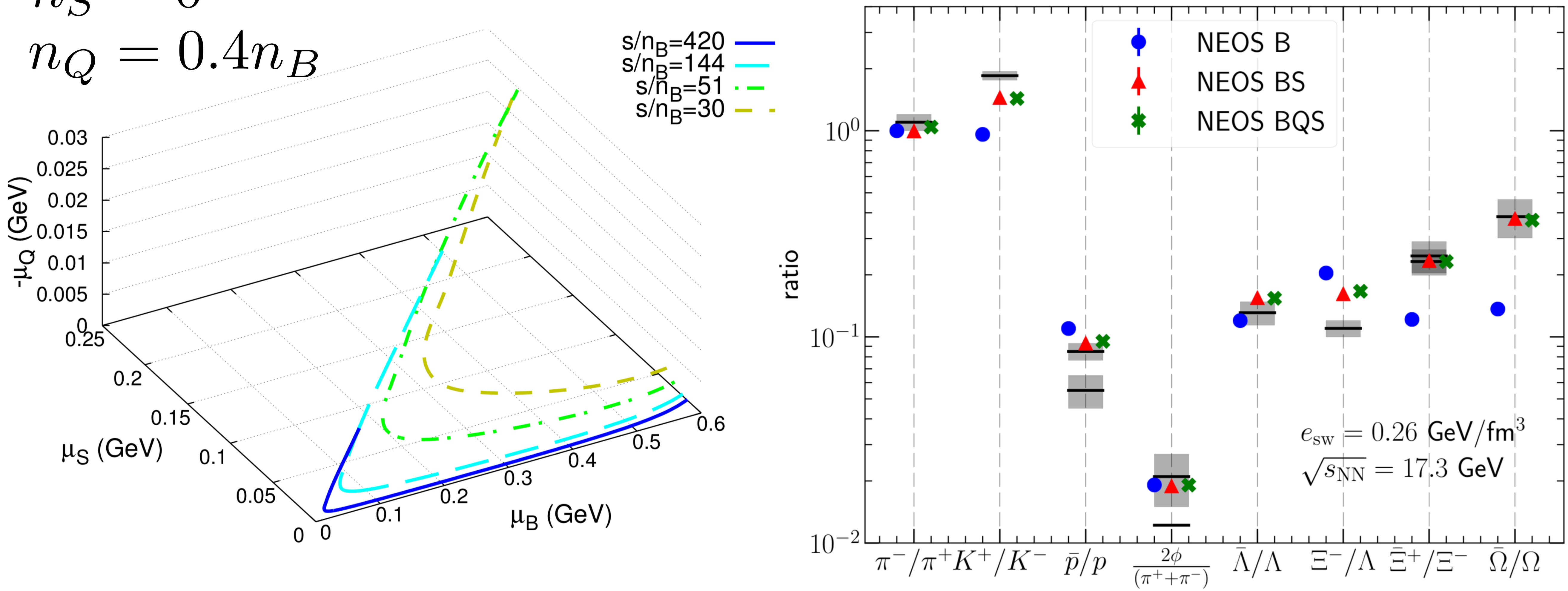

- Lattice QCD EoS has been extended to non-zero net baryon, strangeness, and electric charges and implemented in the hydrodynamic framework

Quantify the baryon stopping

C. Shen and B. Schenke, Nucl. Phys. A982 (2019) 411-414

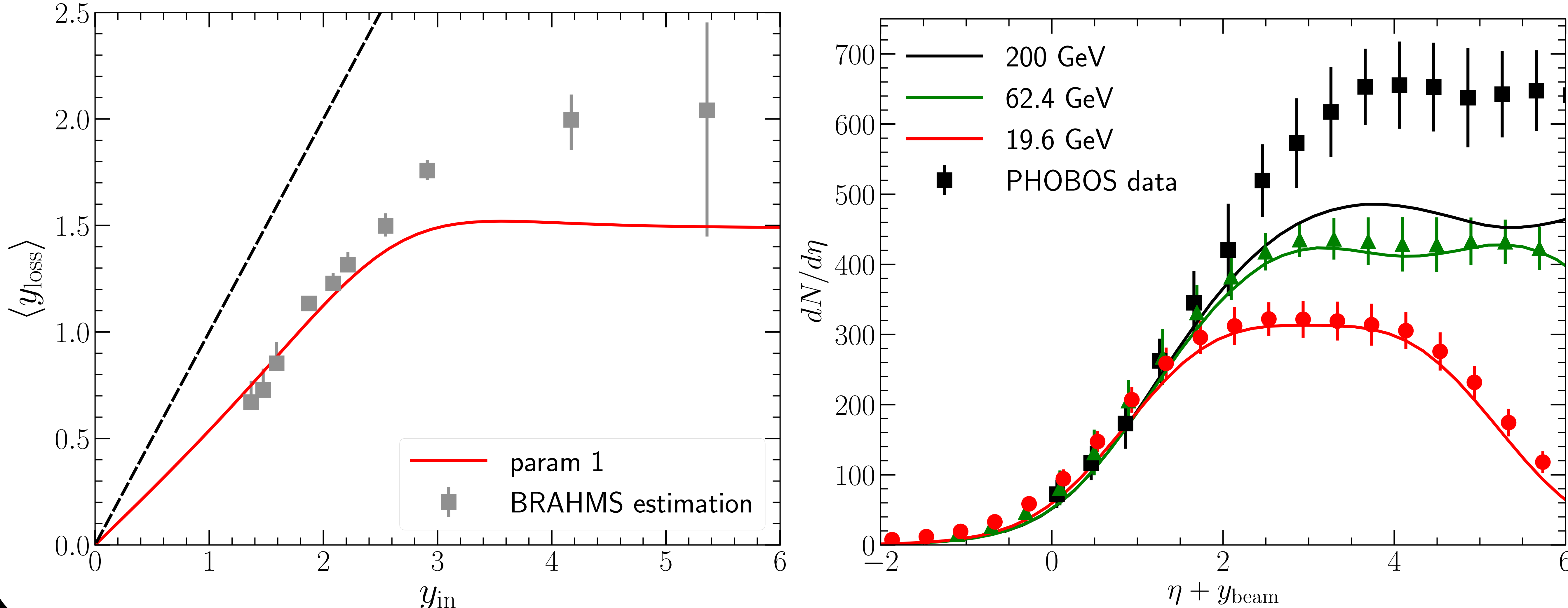

- The charged hadron rapidity distribution is sensitive to the parameterization of the baryon energy loss

Quantify the baryon stopping

C. Shen and B. Schenke, Nucl. Phys. A982 (2019) 411-414

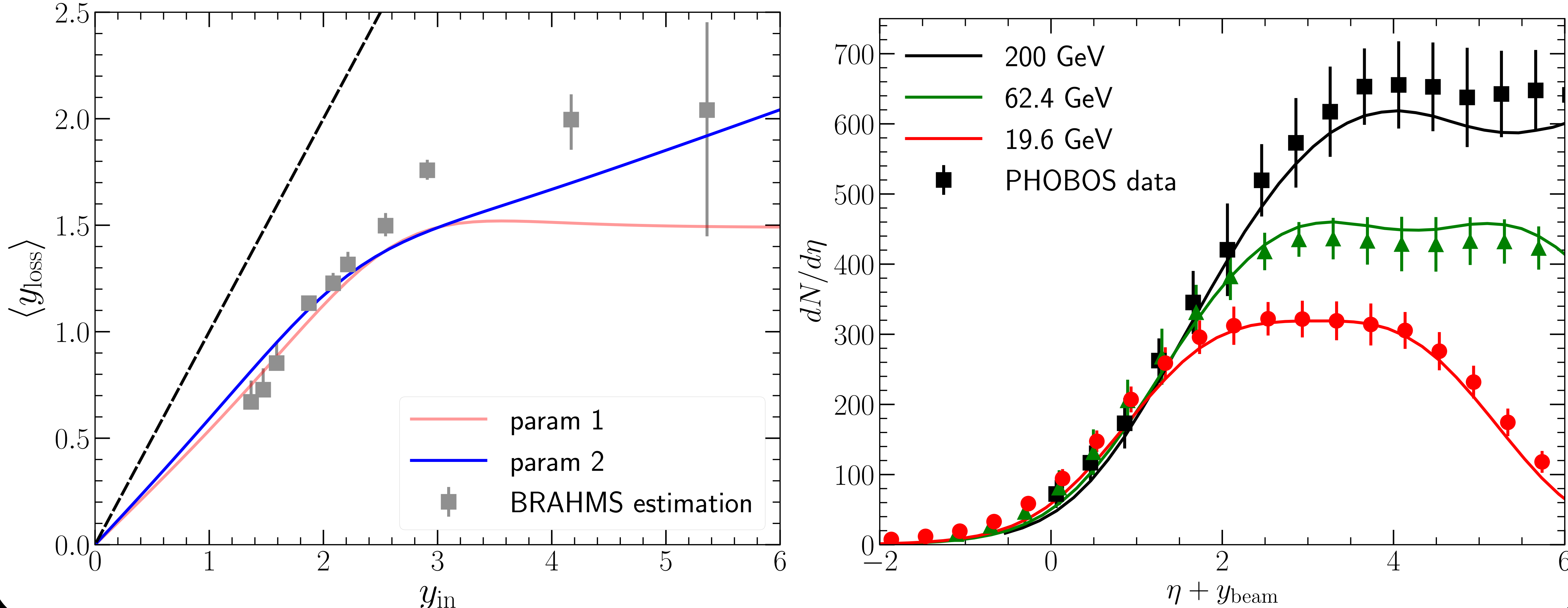

- Understand how the collision energy is converted to particle production

Quantify the baryon stopping

C. Shen and B. Schenke, Phys. Rev. C97 (2018) 024907

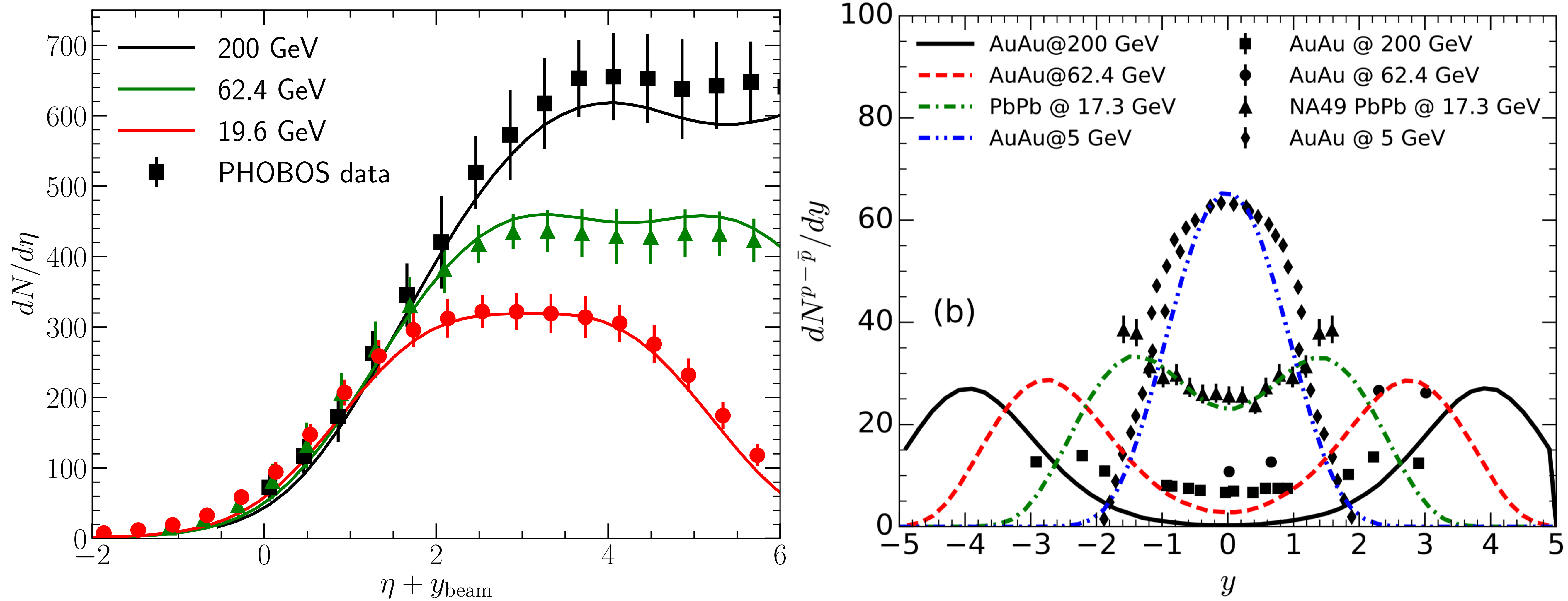

- Our dynamical framework can cover the full collision energy range in RHIC Beam Energy Scan
- Net proton numbers are underestimated at high collision energies

QGP transport property

Shear viscosity	Bulk viscosity	Diffusion
Resistance to deformation $\sim 2\eta\nabla^{\langle\mu}u^{\nu\rangle}$	Resistance to expansion $\sim -\zeta\partial_\mu u^\mu$	particles diffuse out of fluid cell $\sim \kappa_B \nabla^\mu(\mu_B/T)$

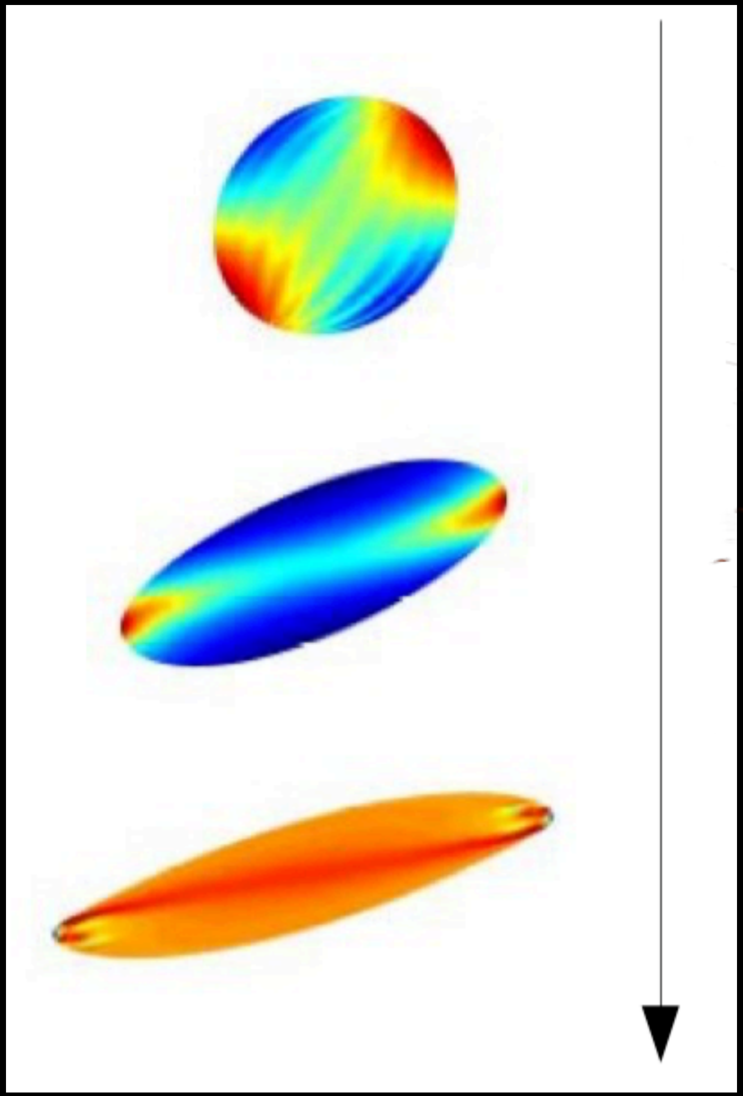

Net baryon diffusion

G. Denicol, C. Gale, S. Jeon, A. Monnai, B. Schenke and C. Shen, Phys. Rev. C98, 034916 (2018)
M. Li and C. Shen, Phys. Rev. C98, 064908 (2018)

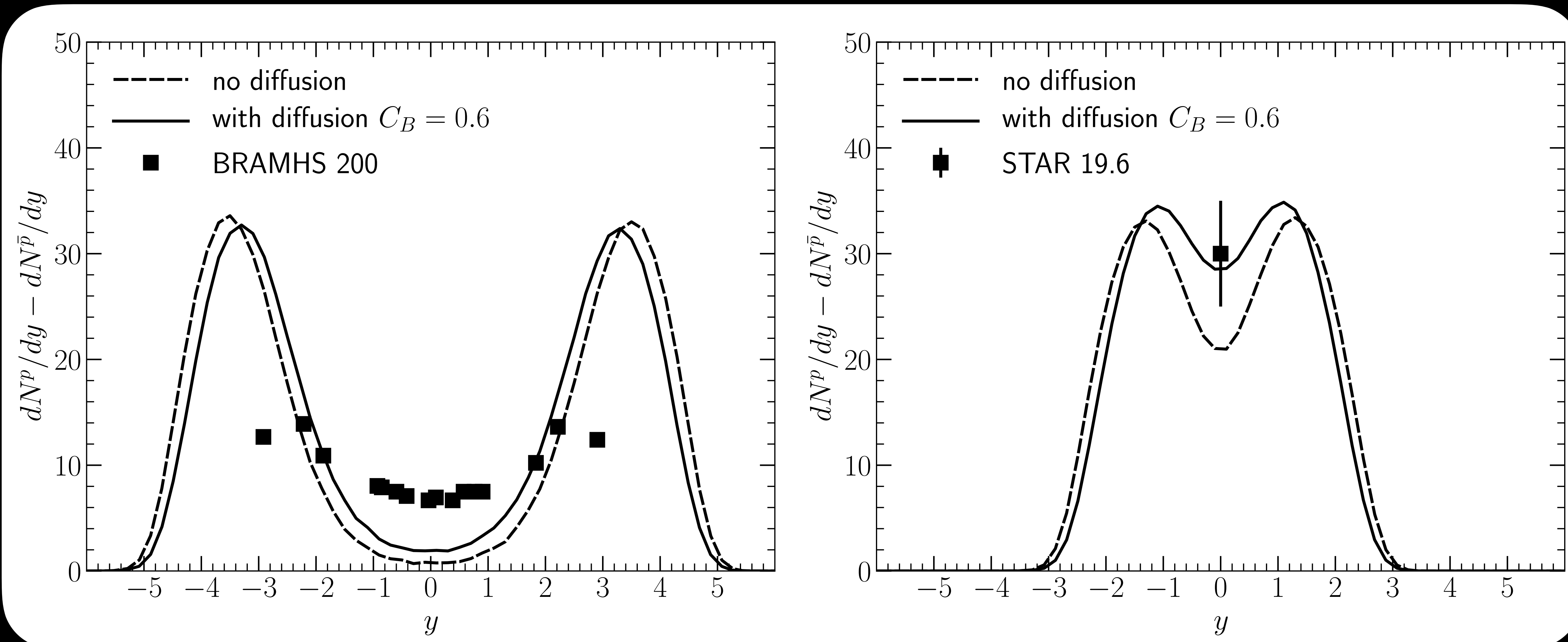

- Net baryon diffusion transports more baryon numbers to the mid-rapidity region

Not enough at high collision energies

Initial state fluctuations of baryon positions

B. Schenke and C. Shen, in preparation

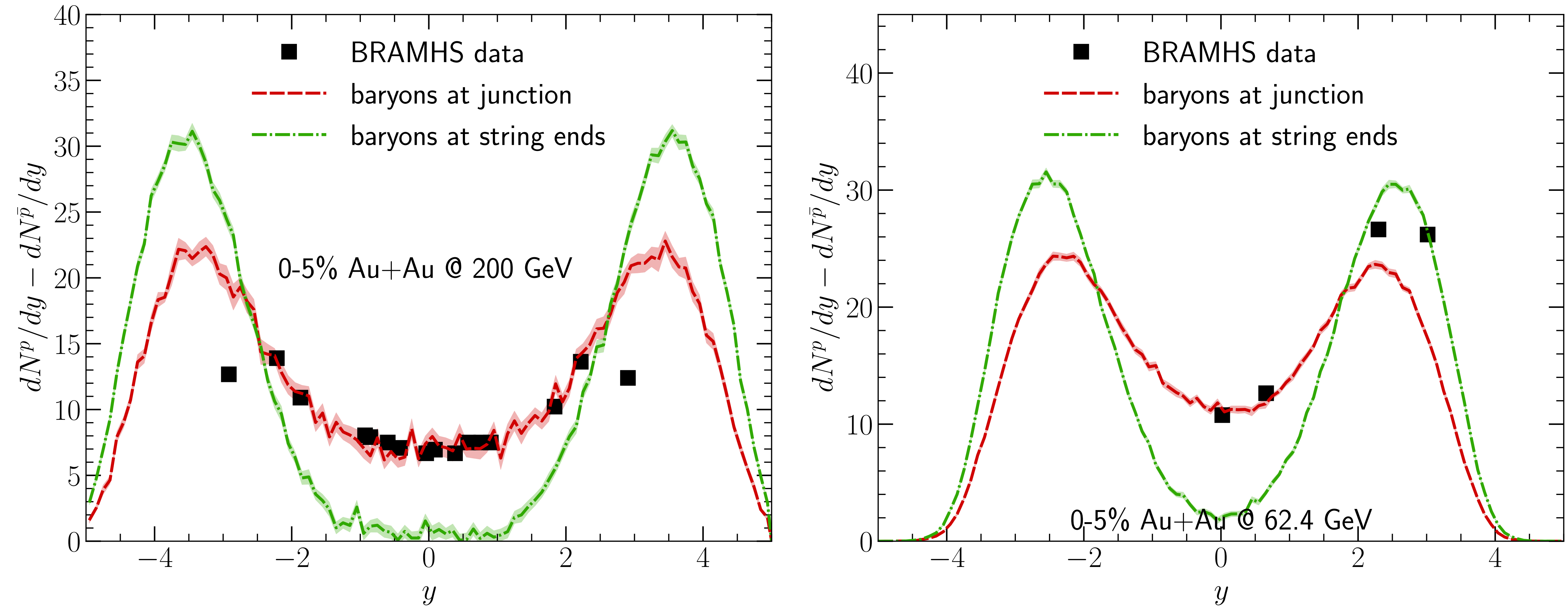

- Allowing the initial baryon density to fluctuate to string junctions improves description at high collision energies

D. Kharzeev, Phys. Lett. B 378, 238 (1996)

Interplay between baryon diffusion and initial fluctuations

Sailing in the QCD phase diagram

C. Shen and B. Schenke, Nucl. Phys. A982 (2019) 411-414

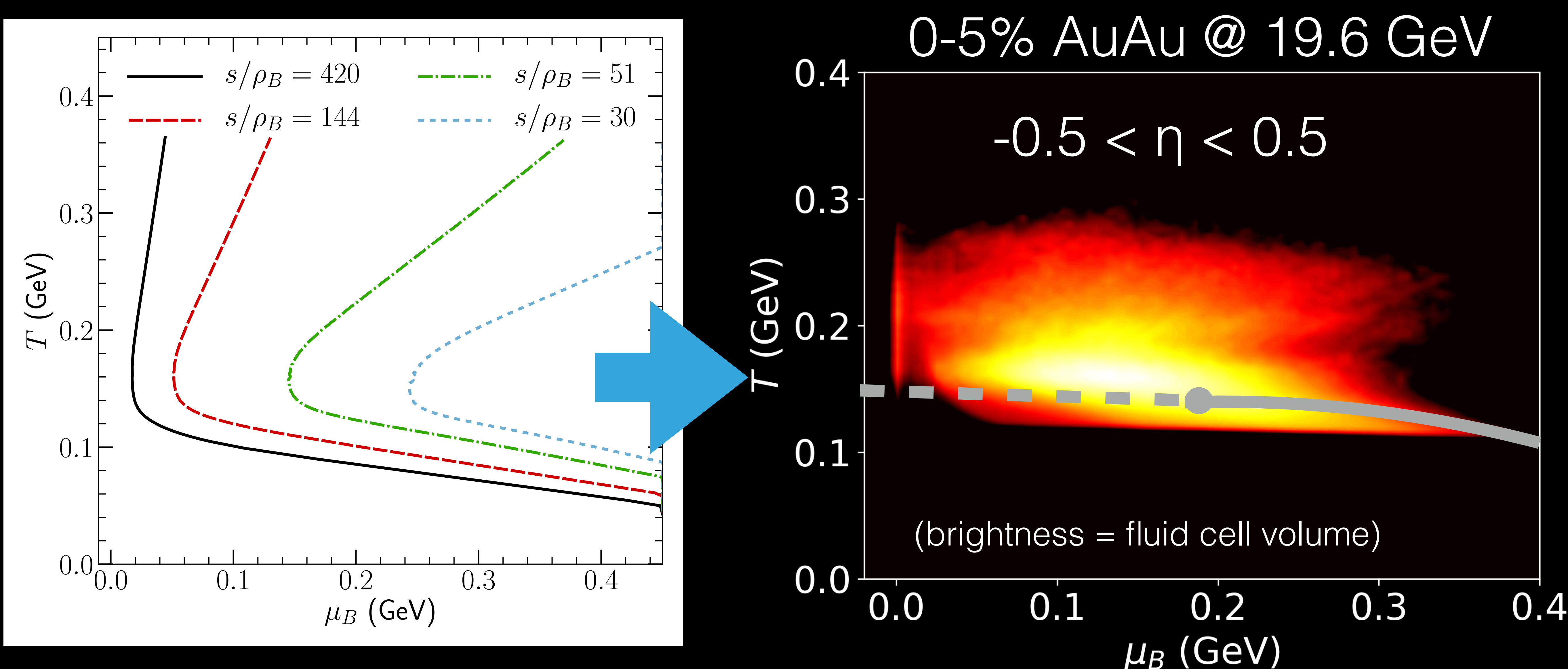

- The fireball trajectory and how fast it flows in the phase diagram are **indispensable** information for the search of the critical point

A baby step towards MUSIC+

C. Shen, in preparation

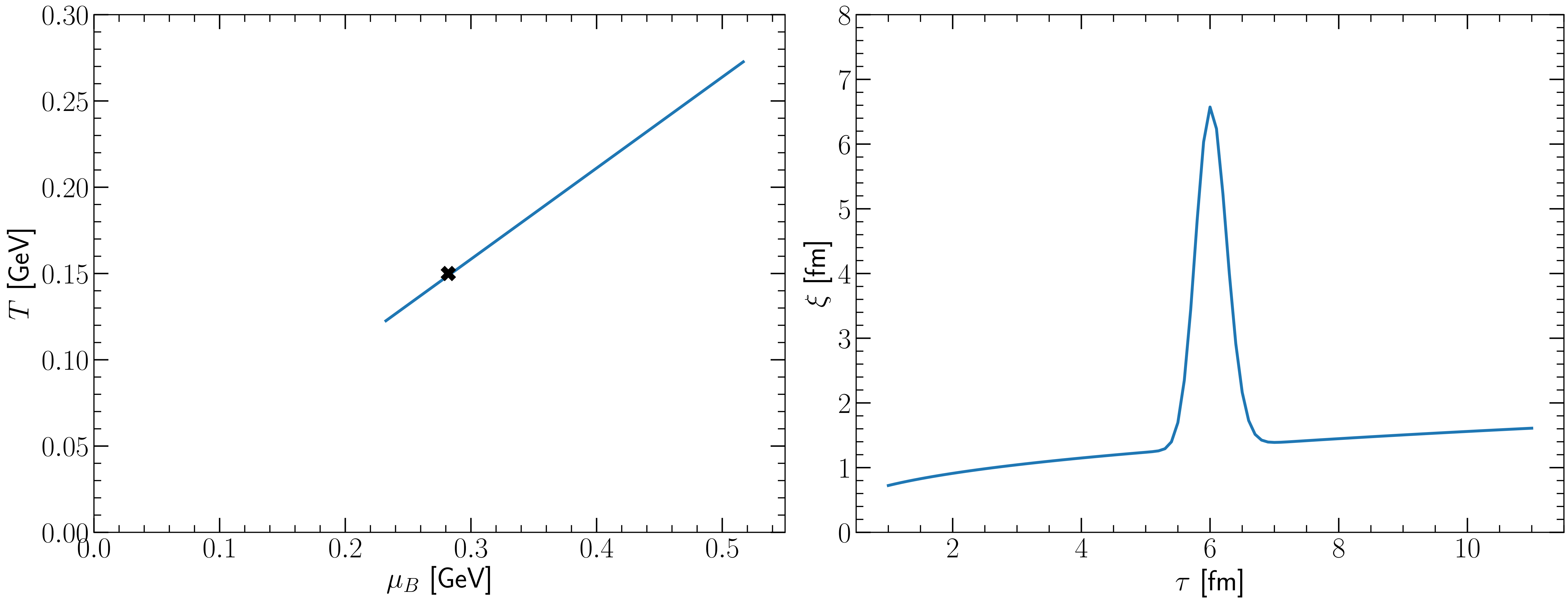

- A "fake" critical point + Bjorken flow expansion
- Evolve the "slow" two-point function $\phi_Q \equiv \left\langle \delta\left(\frac{s}{n}\right) \delta\left(\frac{s}{n}\right) \right\rangle$ according to hydro+ formalism

M. Stephanov and Y. Yin, Phys. Rev. D 98, 036006 (2018)

A baby step towards MUSIC+

C. Shen, in preparation

Approaching the critical point | leaving the critical point

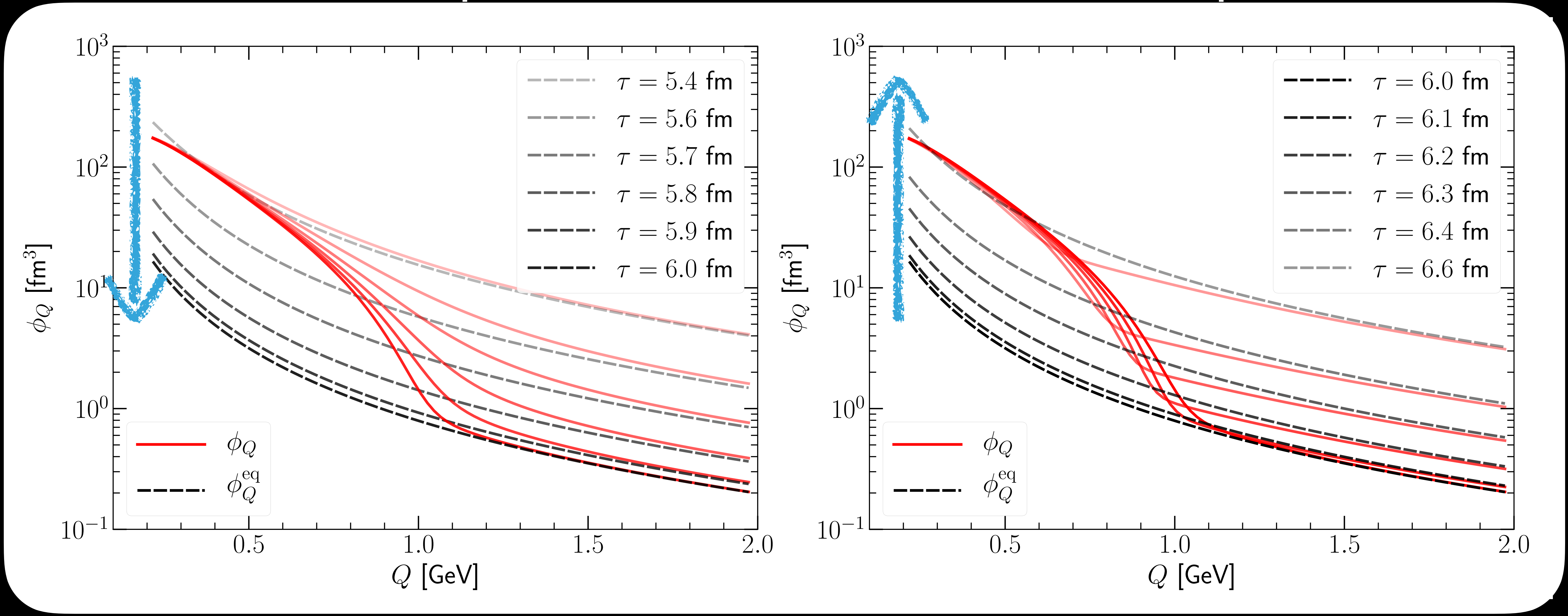

- The two-point function ϕ_Q freeze-out in small Q

Critical slowing down

$$\phi_Q \equiv \left\langle \delta\left(\frac{s}{n}\right)\delta\left(\frac{s}{n}\right)\right\rangle$$

A baby step towards MUSIC+

C. Shen, in preparation

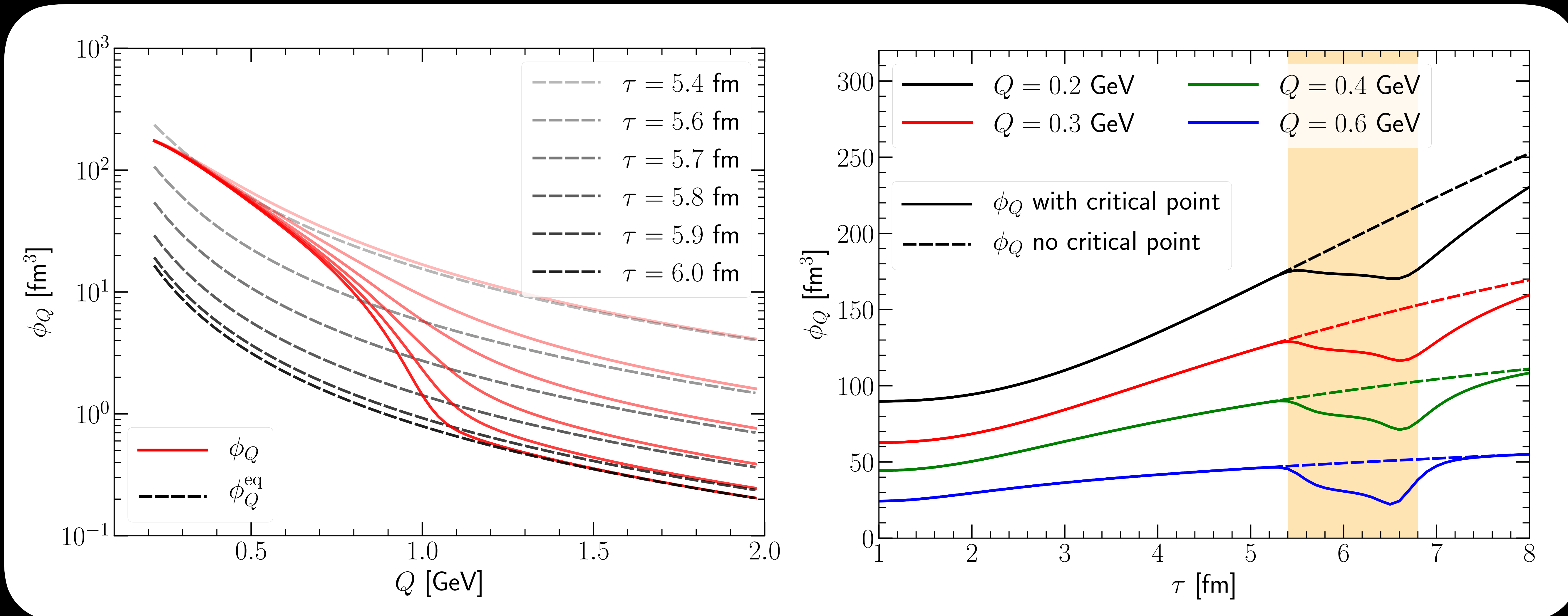

- Chasing the finite memory of the critical point at freeze-out

Critical slowing down

$$\phi_Q \equiv \left\langle \delta\left(\frac{s}{n}\right) \delta\left(\frac{s}{n}\right) \right\rangle$$

Summary and Outlook

- **We developed full-fledged hydrodynamic framework for heavy-ion collisions at RHIC BES energies**

  Elucidating the initial baryon stopping, longitudinal fluctuations, and cross diffusion among multiple conserved charge currents

  Quantitative characterization of Quark-Gluon Plasma transport properties at finite baryon density via Bayesian analysis

- **Realistic mapping of heavy-ion collisions to the QCD phase diagram for the search of critical behaviors at RHIC BES**

  Stochastic hydrodynamics and hydro+
  thermal and critical fluctuations


BACKUP

Initial state fluctuations of baryon positions

B. Schenke and C. Shen, in preparation

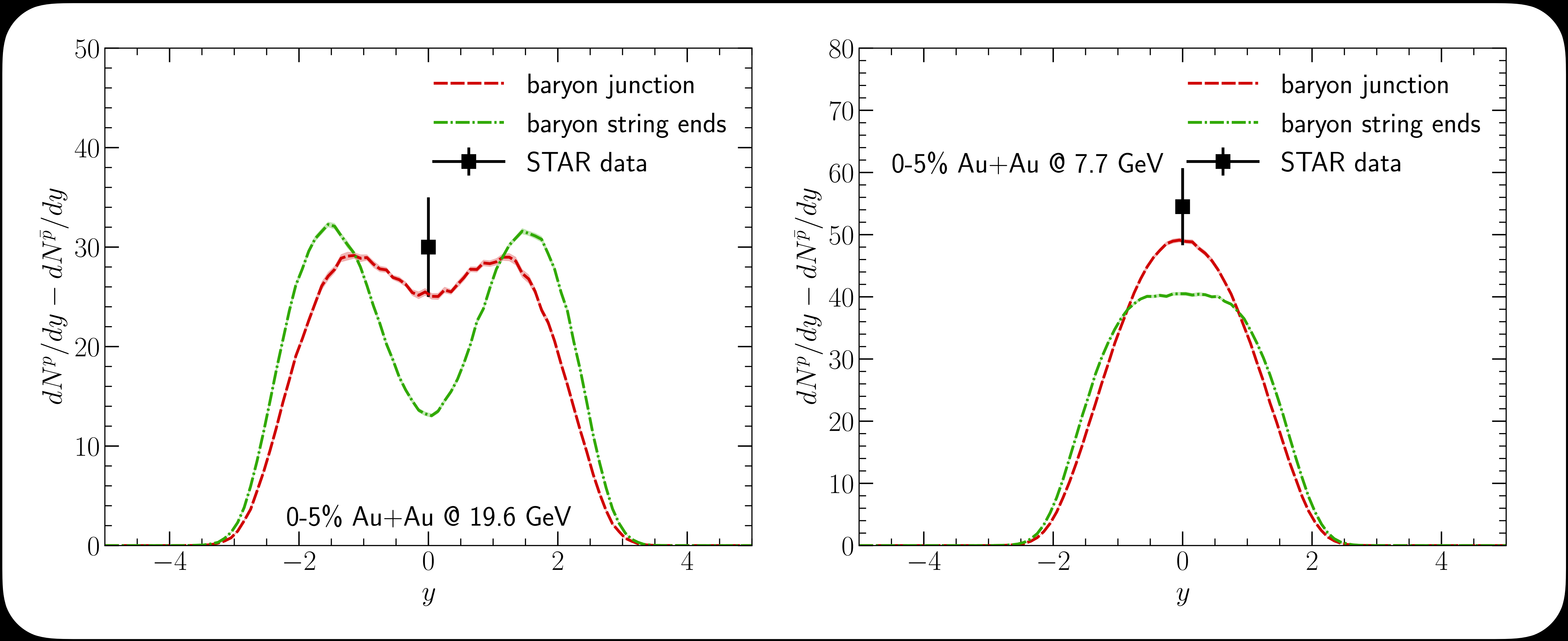

- Including baryon fluctuations at the string junction also improves low collision energy net proton distributions

Interplay between baryon diffusion and initial fluctuations

Sailing in the phase diagram

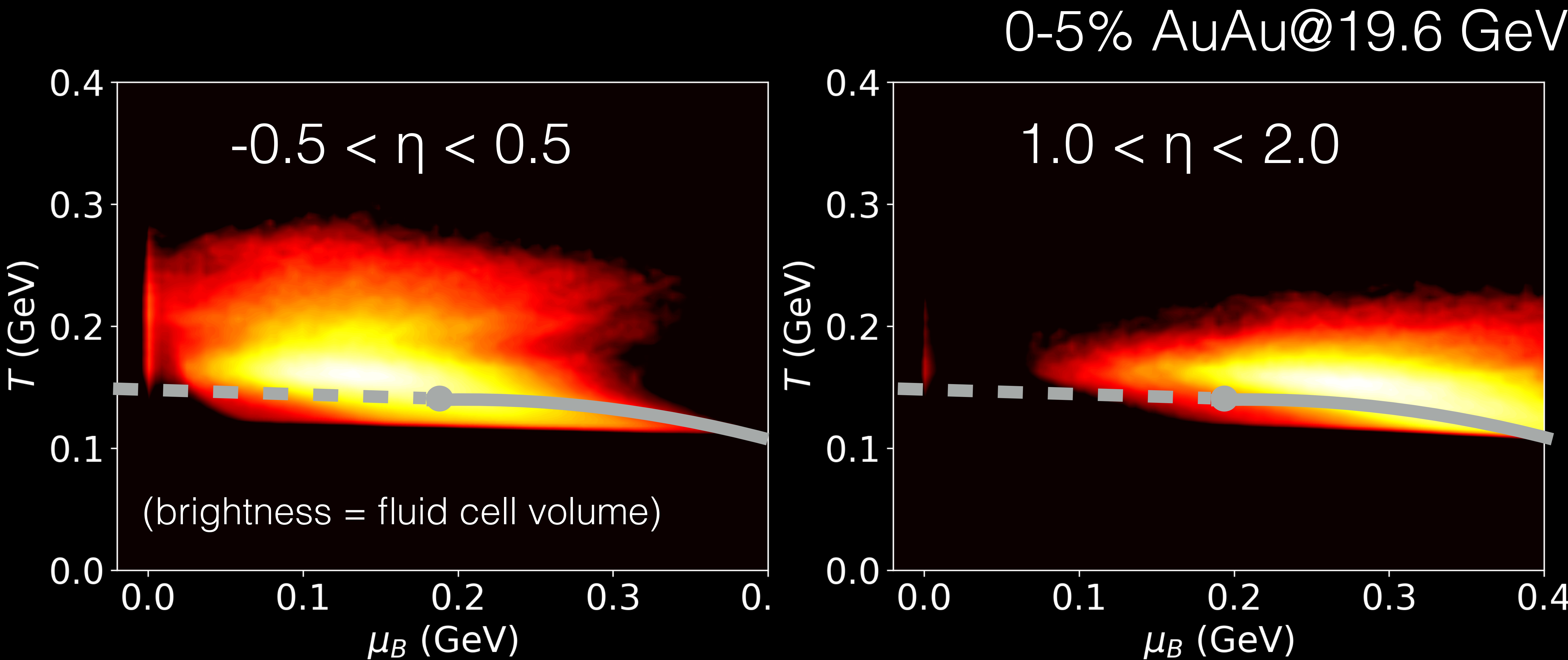

- The fireball trajectory and how fast it flows in the phase diagram are indispensable information for the search of the critical point

EM Tomography in RHIC BES energies

C. Gale, S. Jeon, S. McDonald, J.F. Paquet and C. Shen, Nucl. Phys. A982 (2019) 767-770

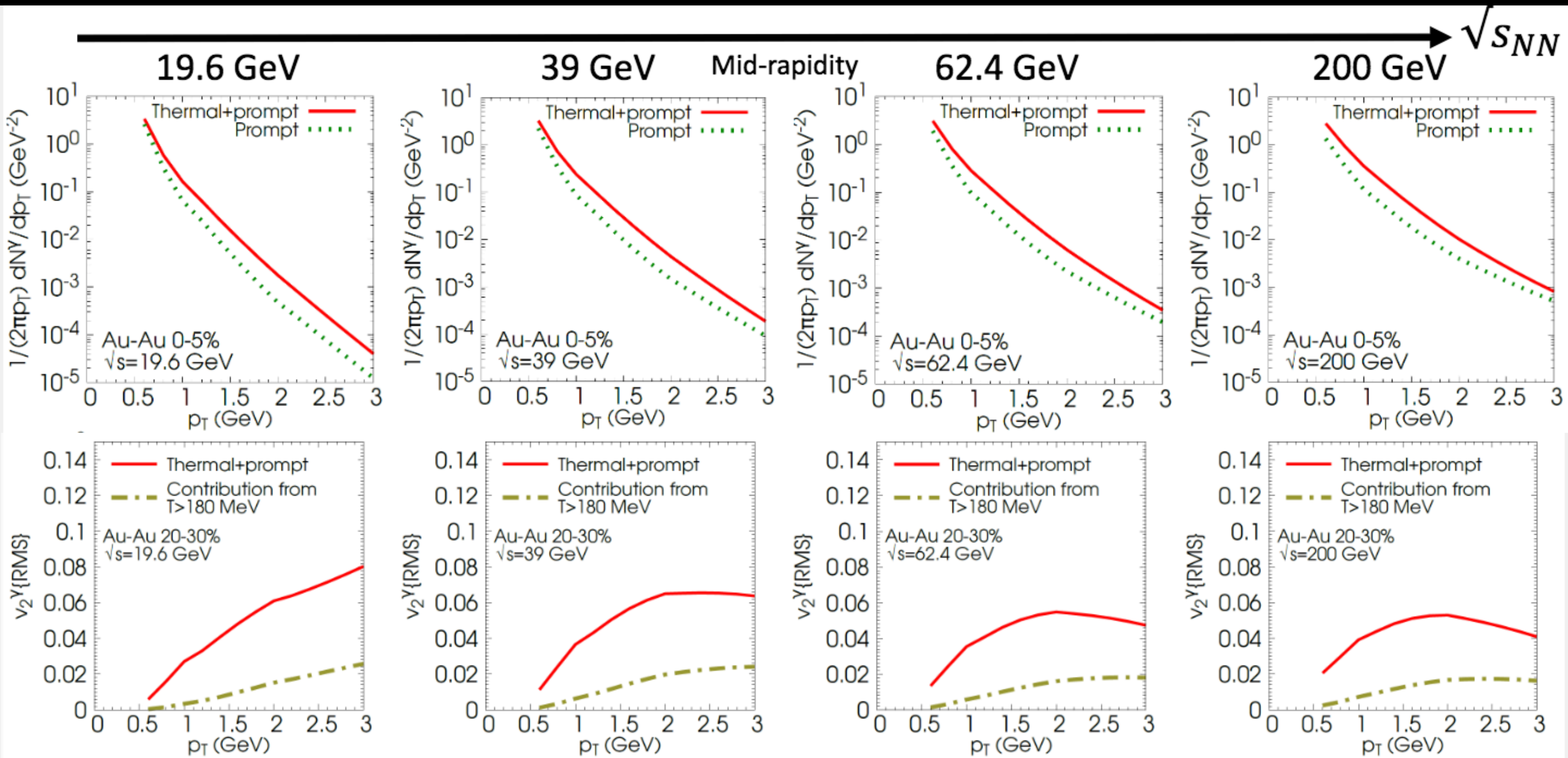

Photons are unique observables to probe early time dynamics

BEST EOS with a critical point

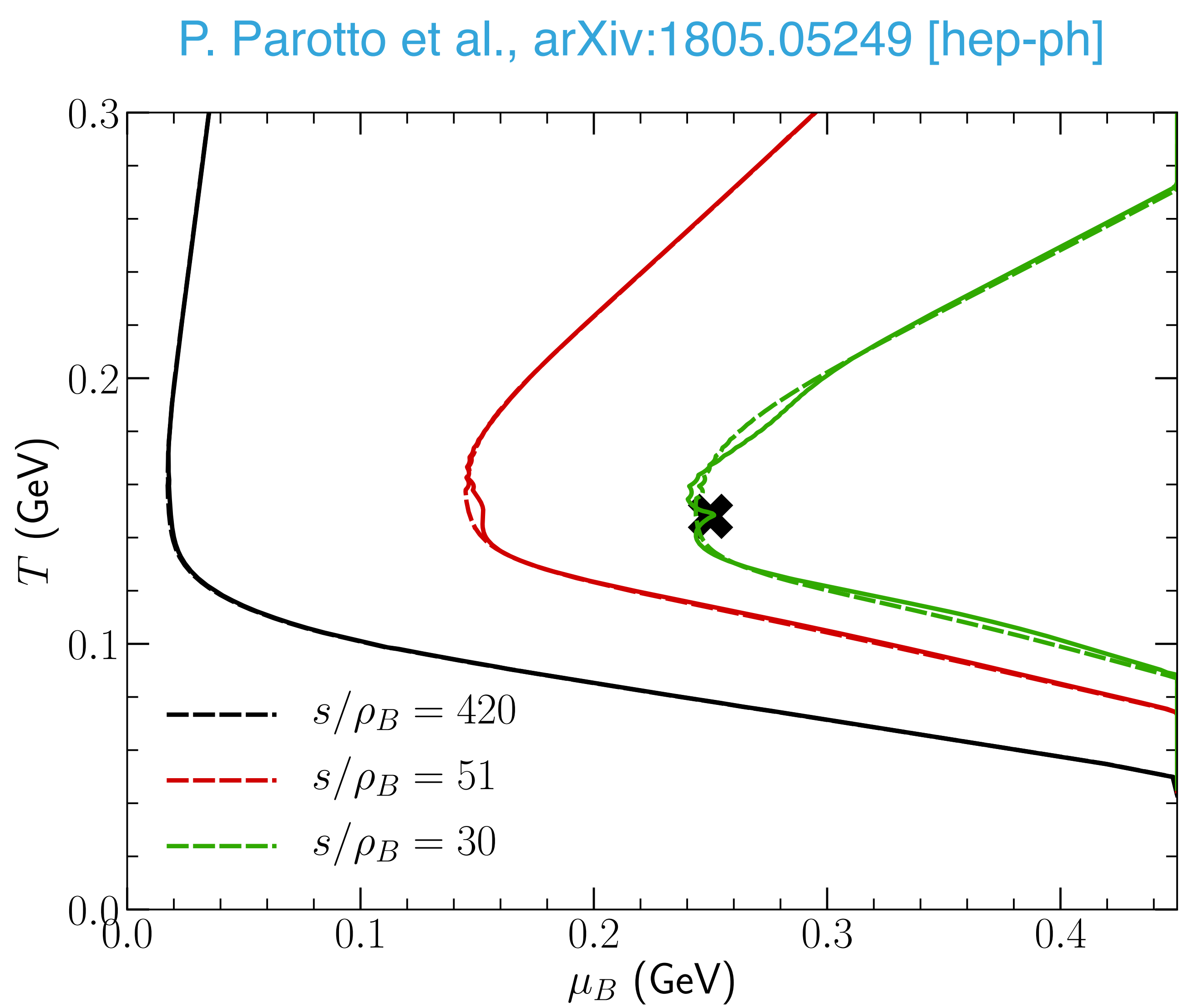

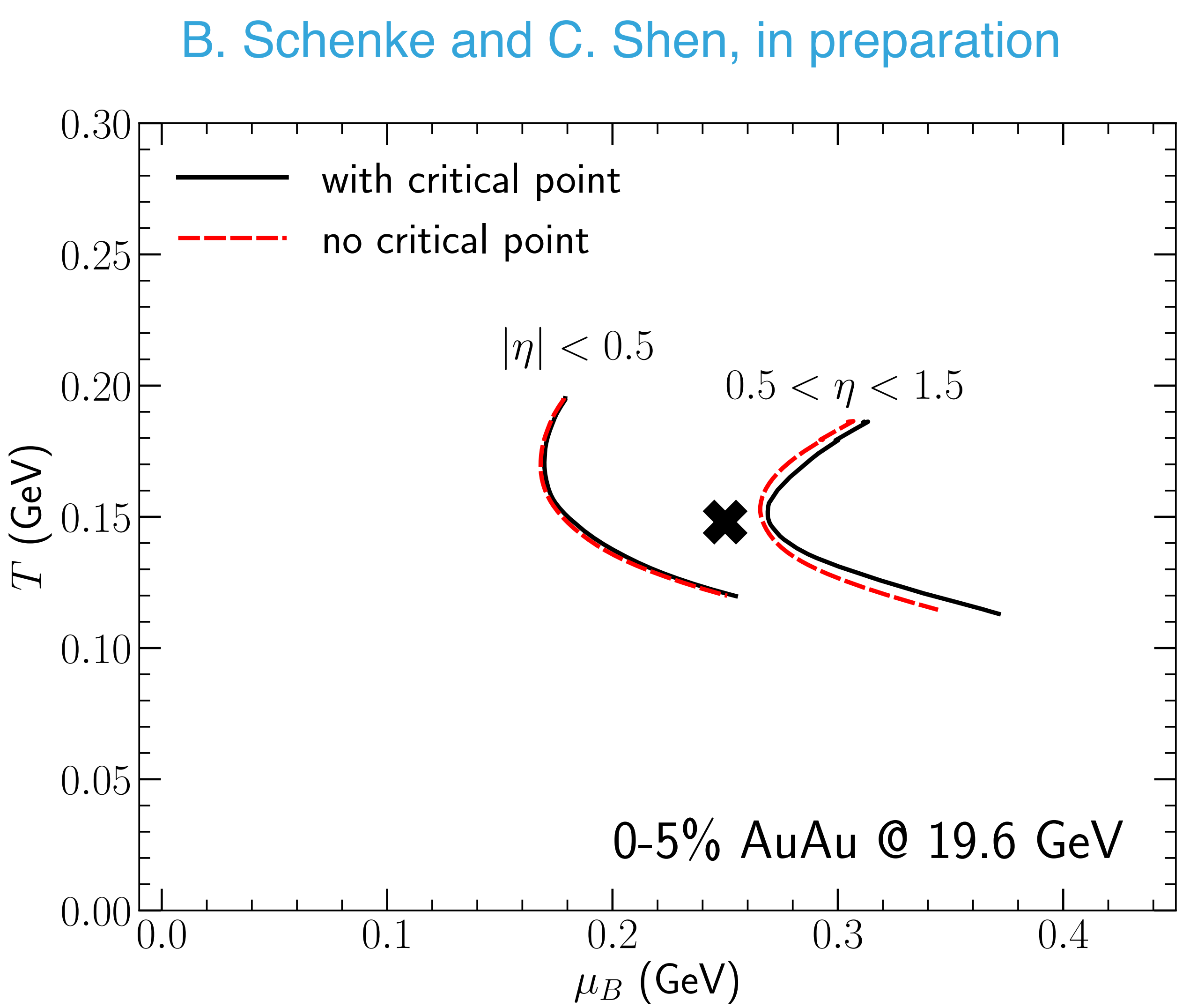

- The BEST EOS is implemented in the state-of-the-art 3D hydrodynamic code (MUSIC)

Visible difference in the fireball trajectories with a critical point

Stochastic hydrodynamics

M. Singh, C. Shen, S. McDonald, S. Jeon and C. Gale, Nucl. Phys. A982, 319 (2019)

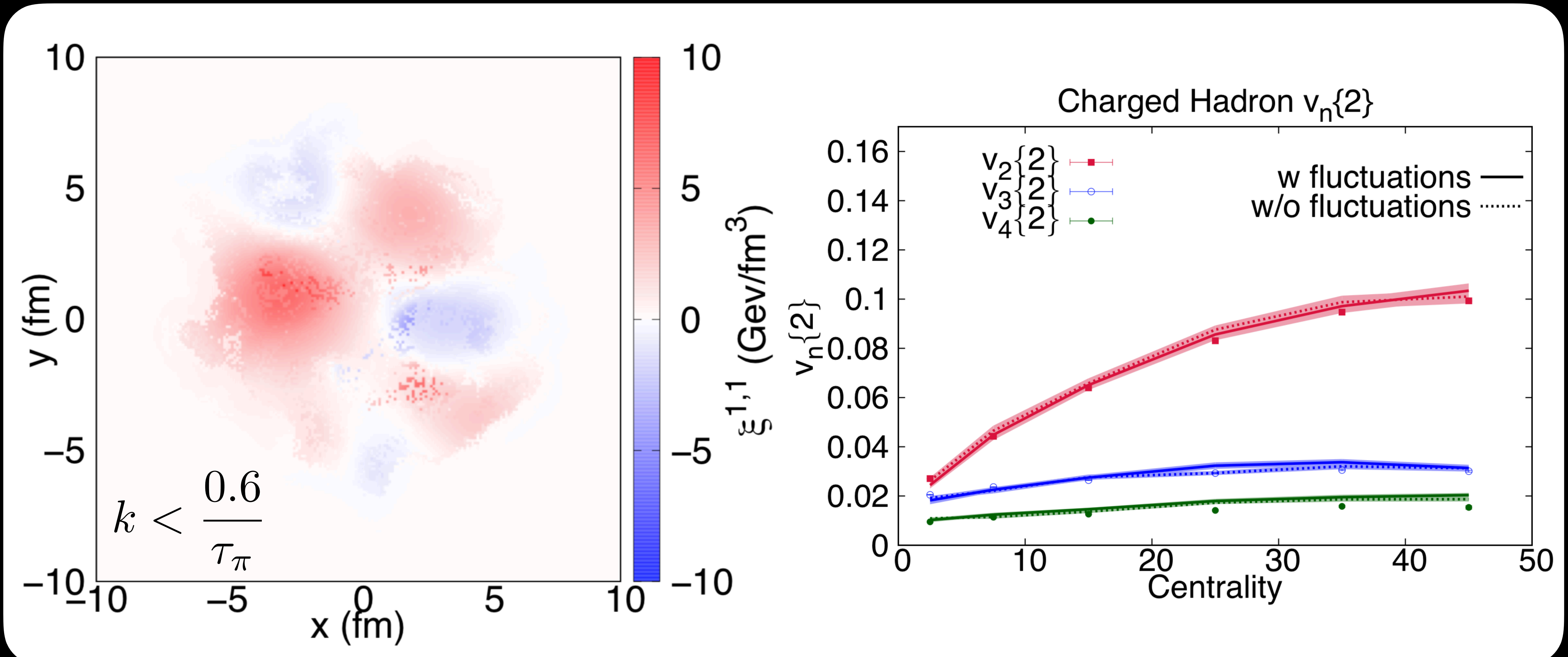

- Thermal fluctuations is implemented in the state-of-the-art viscous hydrodynamic simulations (MUSIC)

First systematic treatment of stochastic noises in 3D hydro

Dynamical initialization based on UrQMD

L. Du, U. Heinz and G. Vujanovic, Nucl. Phys. A982 (2019) 407-410

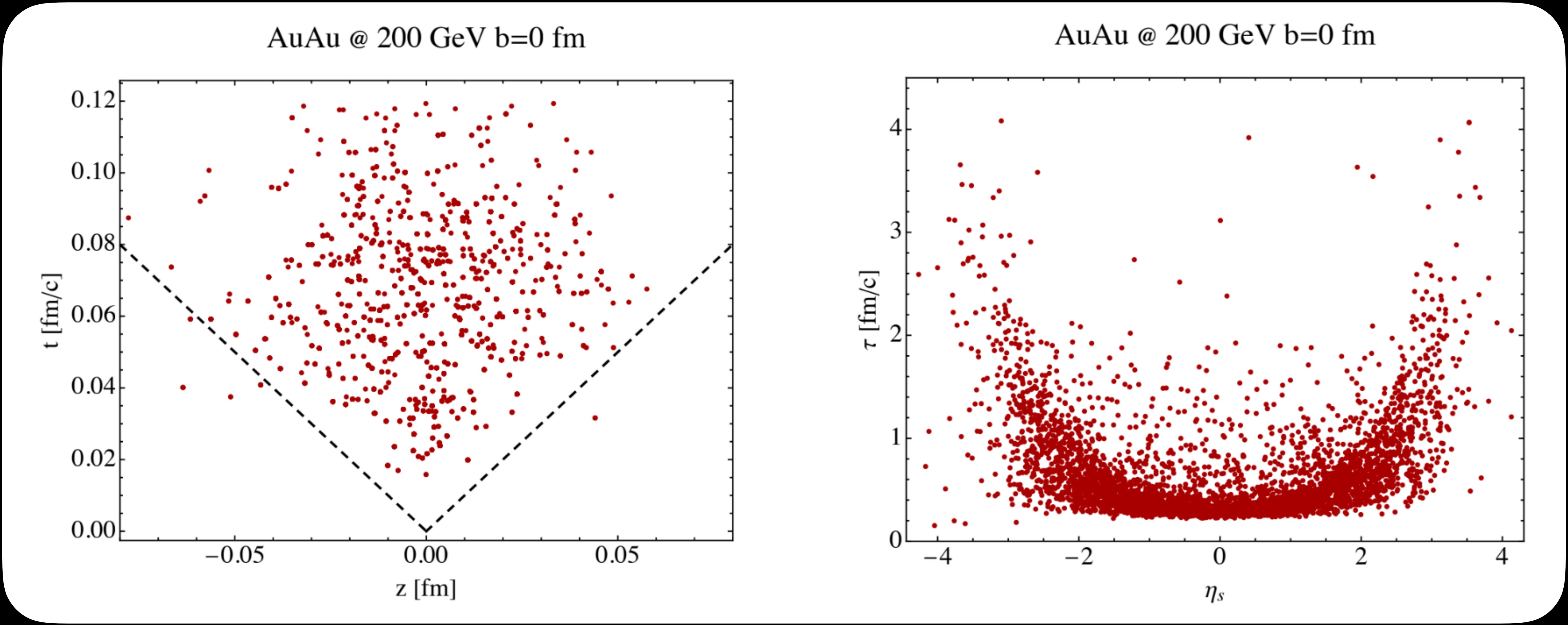

- A similar space-time distribution for the energy-momentum sources
- Contains additional fluctuations from string fragmentation

Energy-momentum space-time distribution

C. Shen and B. Schenke, Phys. Rev. C97 (2018) 024907
L. Du, U. Heinz and G. Vujanovic, Nucl. Phys. A982 (2019) 407-410

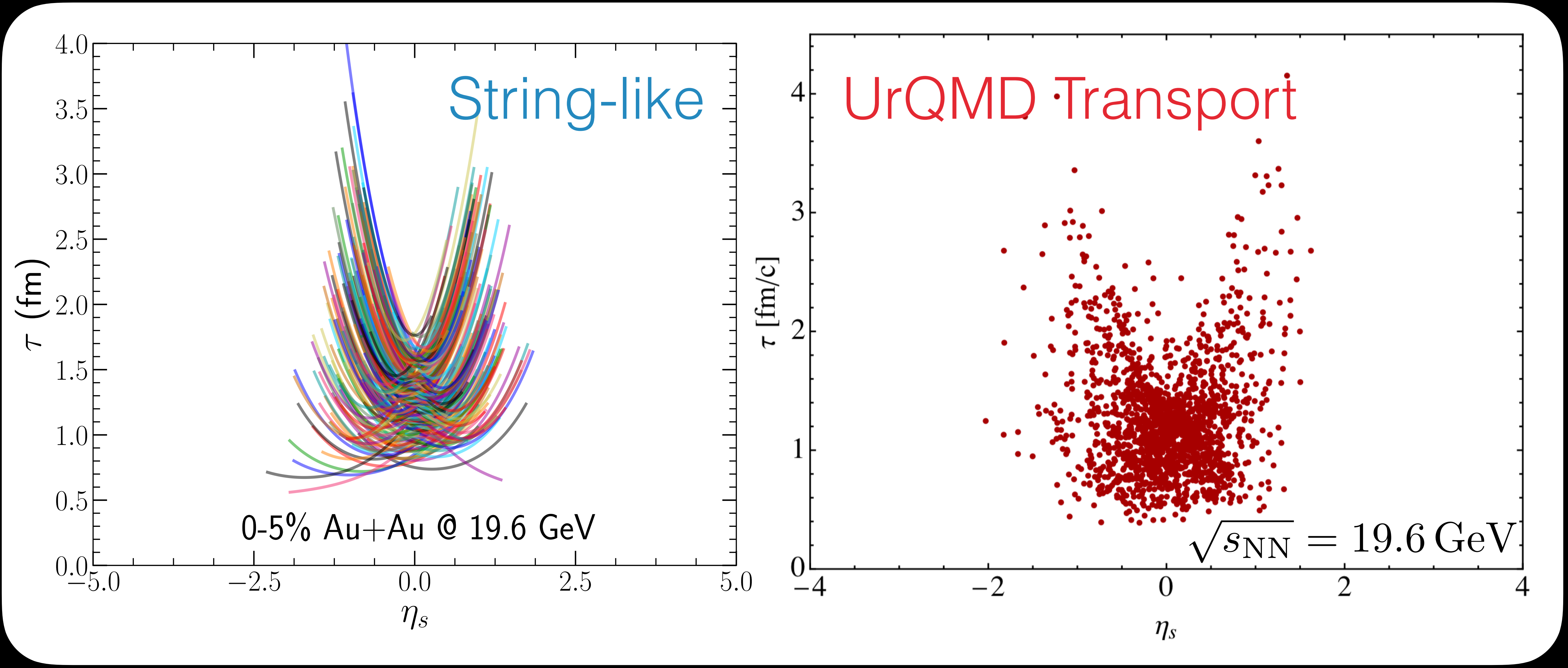

- An extended interaction zone for the energy-momentum sources from the 3D collision geometry

Dynamically interweaves with hydrodynamics

BEST EOS with a critical point

P. Parotto et al., arXiv:1805.05249 [hep-ph]

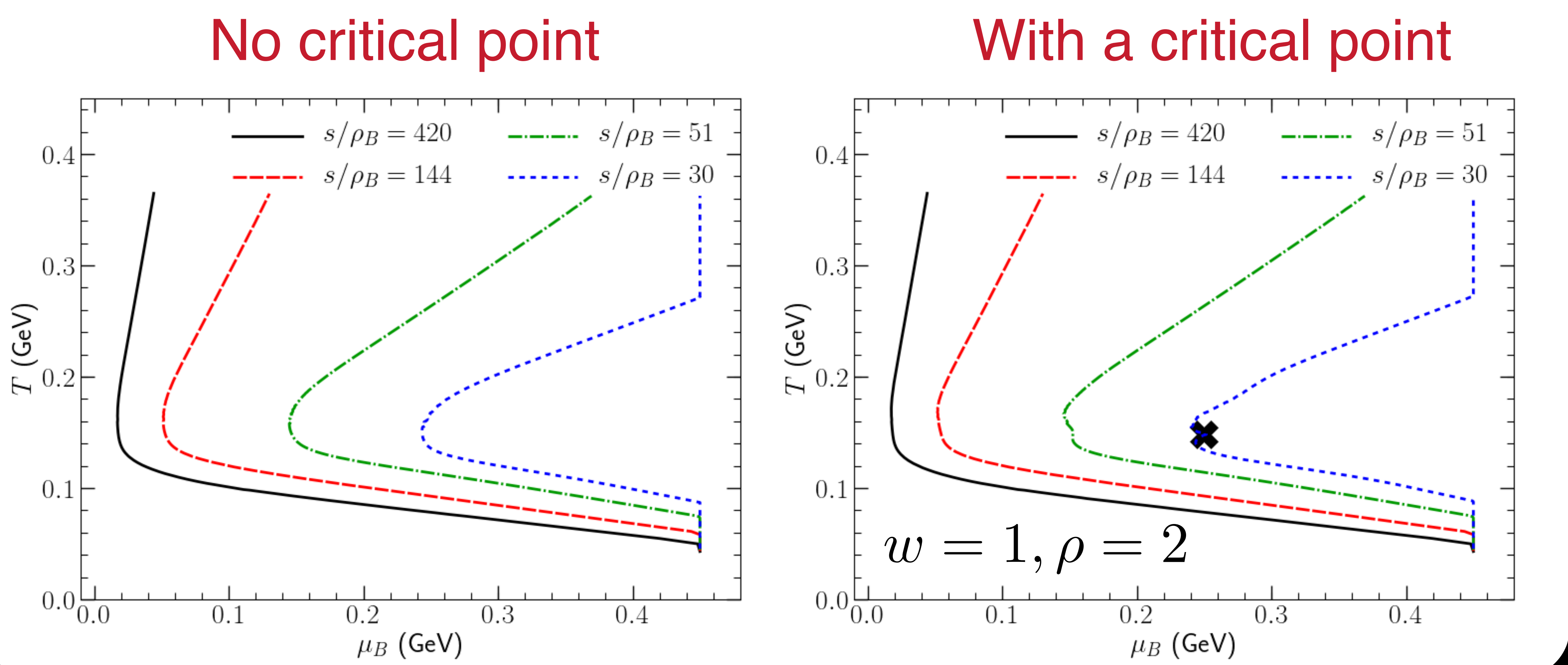

- The BEST EOS is implemented in MUSIC

$$T_{\rm crit} = 148\,\mathrm{MeV}, \mu_{\rm B,crit} = 250\,\mathrm{MeV}$$

BEST EOS with a critical point

P. Parotto et al., arXiv:1805.05249 [hep-ph]

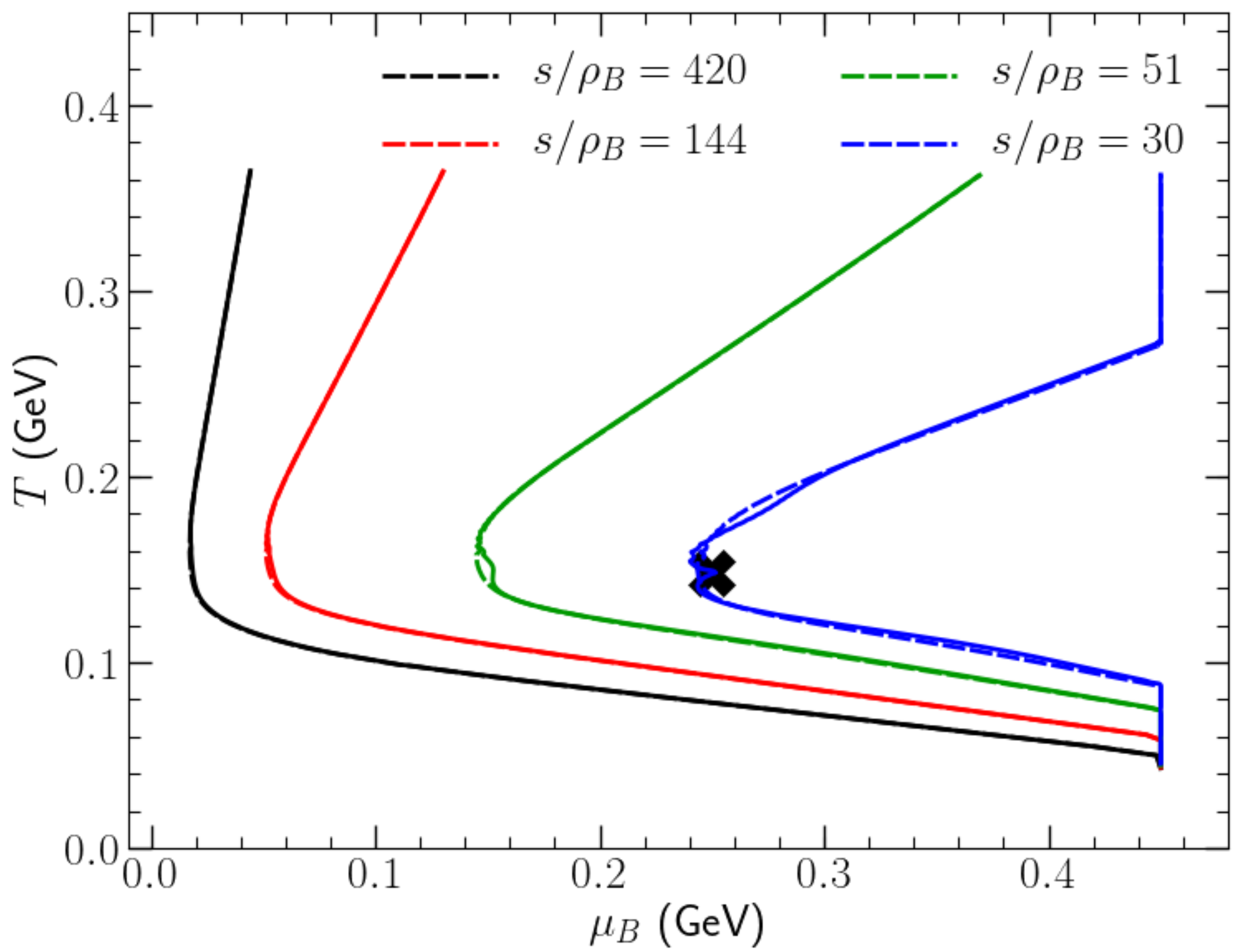

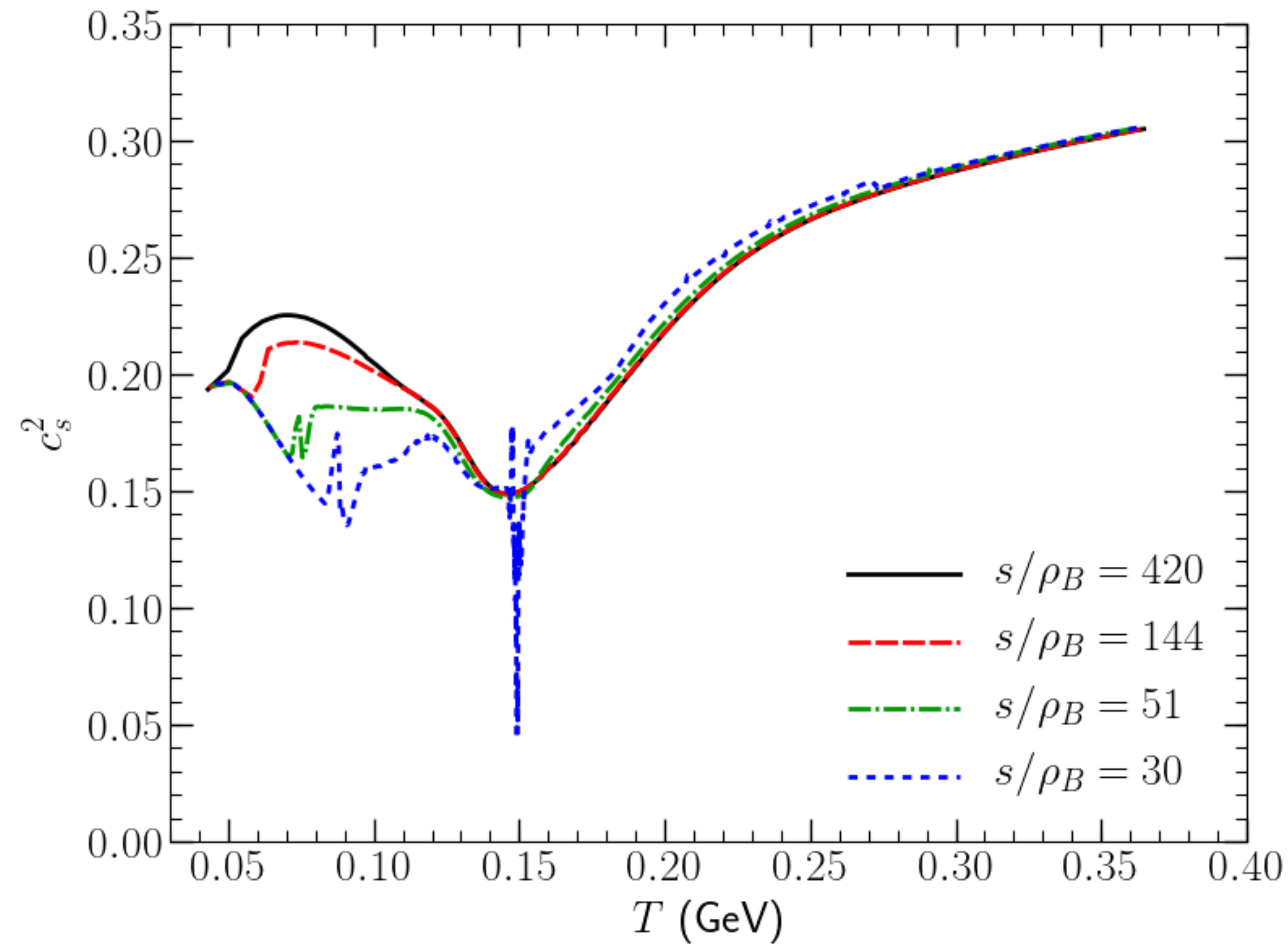

- The BEST EOS is implemented in MUSIC
- The speed of sound dips at the critical point

Dissipative hydrodynamics

Energy momentum tensor

$$T^{\mu\nu} = e u^\mu u^\nu - (P + \Pi)\Delta^{\mu\nu} + \pi^{\mu\nu}$$

$$\Delta^{\mu\nu} = g^{\mu\nu} - u^\mu u^\nu$$

Conserved currents

$$J^\mu = n u^\mu + q^\mu$$

Equations of motion

$$\begin{array}{l} \partial_\mu T^{\mu\nu} = 0 \\ \partial_\mu J^\mu = 0 \end{array} \quad + \quad P(e, n)$$

Dissipative quantities are evolved with 2nd order Israel-Stewart type of equations

At Navier-Stokes limit,

$$\pi^{\mu\nu} \sim 2\eta \nabla^{\langle\mu} u^{\nu\rangle} \quad \Pi \sim -\zeta \partial_\mu u^\mu \quad q^\mu \sim \kappa \nabla^\mu \frac{\mu}{T}$$

$$\nabla^\mu = \Delta^{\mu\nu}\partial_\nu$$

Hydrodynamics

Energy momentum tensor

$$T^{\mu\nu} = e u^\mu u^\nu - (P + \Pi)\Delta^{\mu\nu} + \pi^{\mu\nu}$$

$$\partial_\mu T^{\mu\nu} = T^{\mu\nu}{}_{;\mu} = 0$$

$$\Delta^{\mu\nu} = g^{\mu\nu} - u^\mu u^\nu$$

Conserved currents

$$J^\mu = n u^\mu + q^\mu$$

$$\partial_\mu J^\mu = 0$$

$$D = u^\mu \partial_\mu$$

$$\nabla^\mu = \Delta^{\mu\nu}\partial_\nu$$

$$\theta = \partial_\mu u^\mu$$

Dissipative part:

$$\Delta^{\mu\nu}_{\alpha\beta} D\pi^{\alpha\beta} = -\frac{1}{\tau_\pi}(\pi^{\mu\nu} - 2\eta\sigma^{\mu\nu}) - \frac{\delta_{\pi\pi}}{\tau_\pi}\pi^{\mu\nu}\theta - \frac{\tau_{\pi\pi}}{\tau_\pi}\pi^{\lambda\langle\mu}\sigma^{\nu\rangle}{}_\lambda + \frac{\phi_7}{\tau_\pi}\pi_\alpha^{\langle\mu}\pi^{\nu\rangle\alpha} - \frac{\tau_{\pi\pi}}{\tau_\pi}\pi_\alpha^{\langle\mu}\sigma^{\nu\rangle\alpha} + \frac{\lambda_{\pi\Pi}}{\tau_\pi}\Pi\sigma^{\mu\nu}$$

$$D\Pi = -\frac{1}{\tau_\Pi}(\Pi + \zeta\theta) - \frac{\delta_{\Pi\Pi}}{\tau_\Pi}\Pi\theta + \frac{\lambda_{\Pi\pi}}{\tau_\Pi}\pi^{\mu\nu}\sigma_{\mu\nu}$$

$$\Delta^{\mu\nu} Dq_\nu = -\frac{1}{\tau_q}\left(q^\mu - \kappa\nabla^\mu\frac{\mu_B}{T}\right) - \frac{\delta_{qq}}{\tau_q}q^\mu\theta - \frac{\lambda_{qq}}{\tau_q}q_\nu\sigma^{\mu\nu}$$

Transport coefficients

Dissipative part: (relaxation time approximation)

$$\Delta^{\mu\nu}_{\alpha\beta} D\pi^{\alpha\beta} = -\frac{1}{\tau_\pi}(\pi^{\mu\nu} - 2\eta\sigma^{\mu\nu}) - \frac{\delta_{\pi\pi}}{\tau_\pi}\pi^{\mu\nu}\theta - \frac{\tau_{\pi\pi}}{\tau_\pi}\pi^{\lambda\langle\mu}\sigma^{\nu\rangle}{}_\lambda + \frac{\phi_7}{\tau_\pi}\pi^{\langle\mu}_\alpha\pi^{\nu\rangle\alpha}$$

$$\Delta^{\mu\nu} Dq_\nu = -\frac{1}{\tau_q}\left(q^\mu - \kappa\nabla^\mu\frac{\mu_B}{T}\right) - \frac{\delta_{qq}}{\tau_q}q^\mu\theta - \frac{\lambda_{qq}}{\tau_q}q_\nu\sigma^{\mu\nu}$$

With non-zero μ, we choose $\tau_\pi = \tau_q = \dfrac{0.4}{T}$ $\quad \dfrac{\eta T}{e+\mathcal{P}} = 0.08$

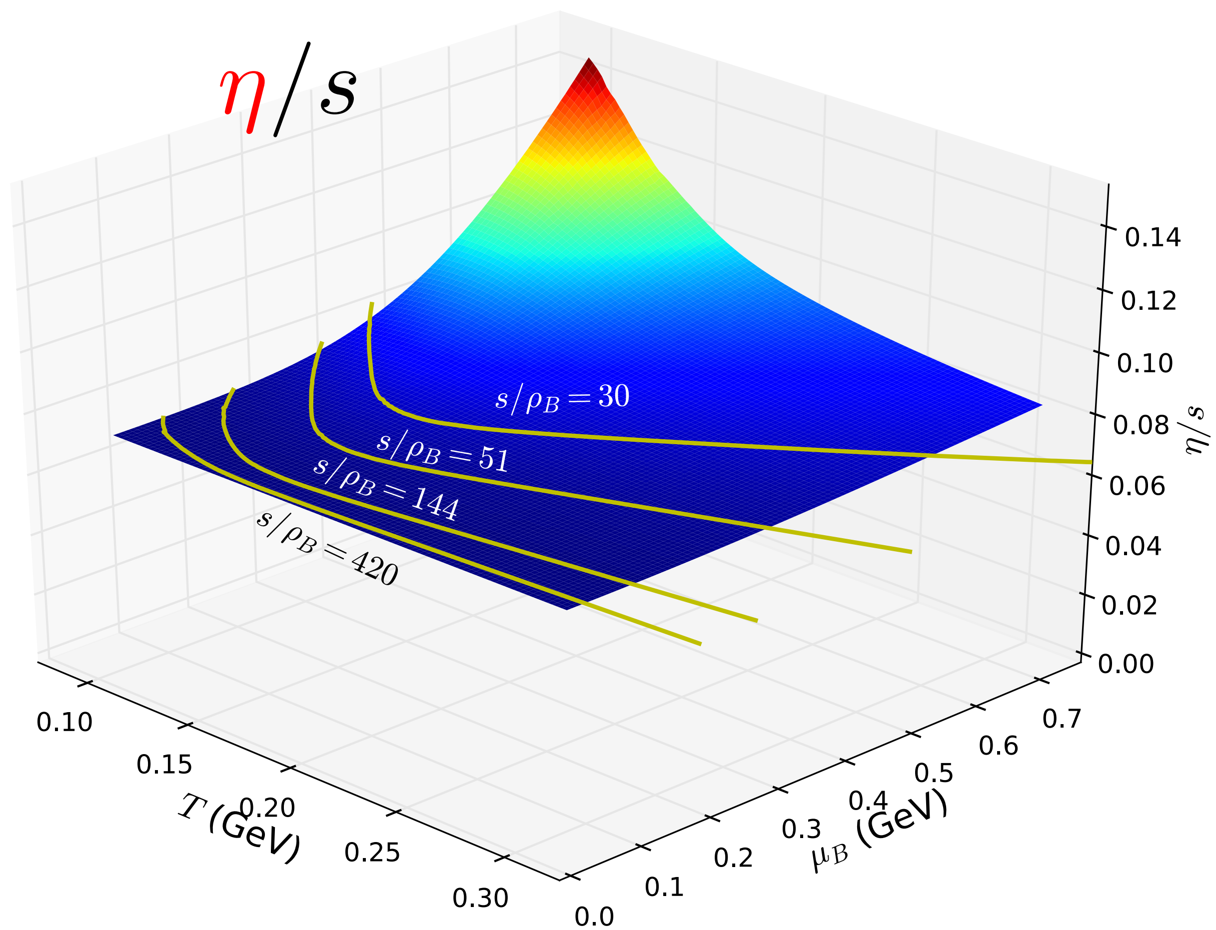

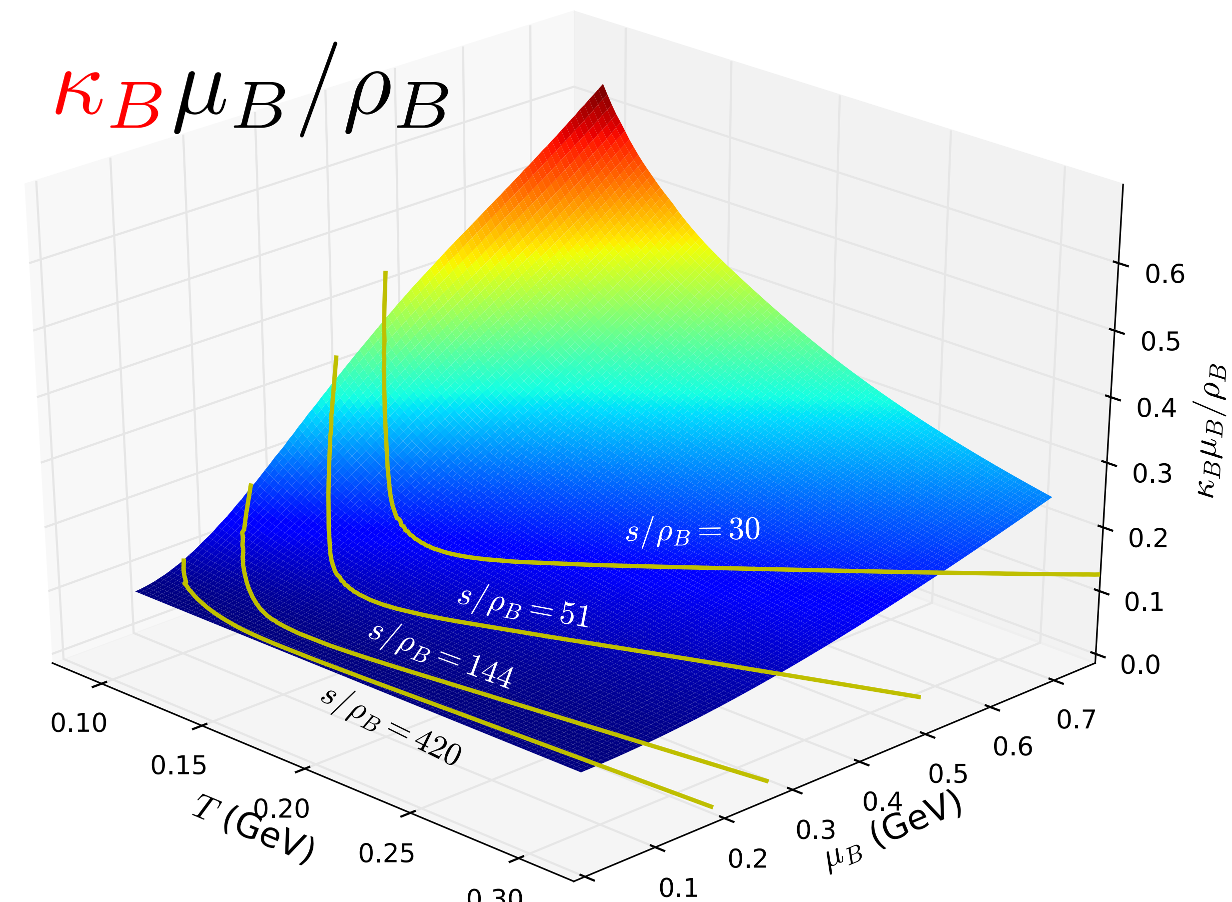

$$\kappa_B = \frac{C_B}{T}\rho_B\left(\frac{1}{3}\coth\left(\frac{\mu_B}{T}\right) - \frac{\rho_B T}{e+P}\right)$$

Longitudinal fluctuations

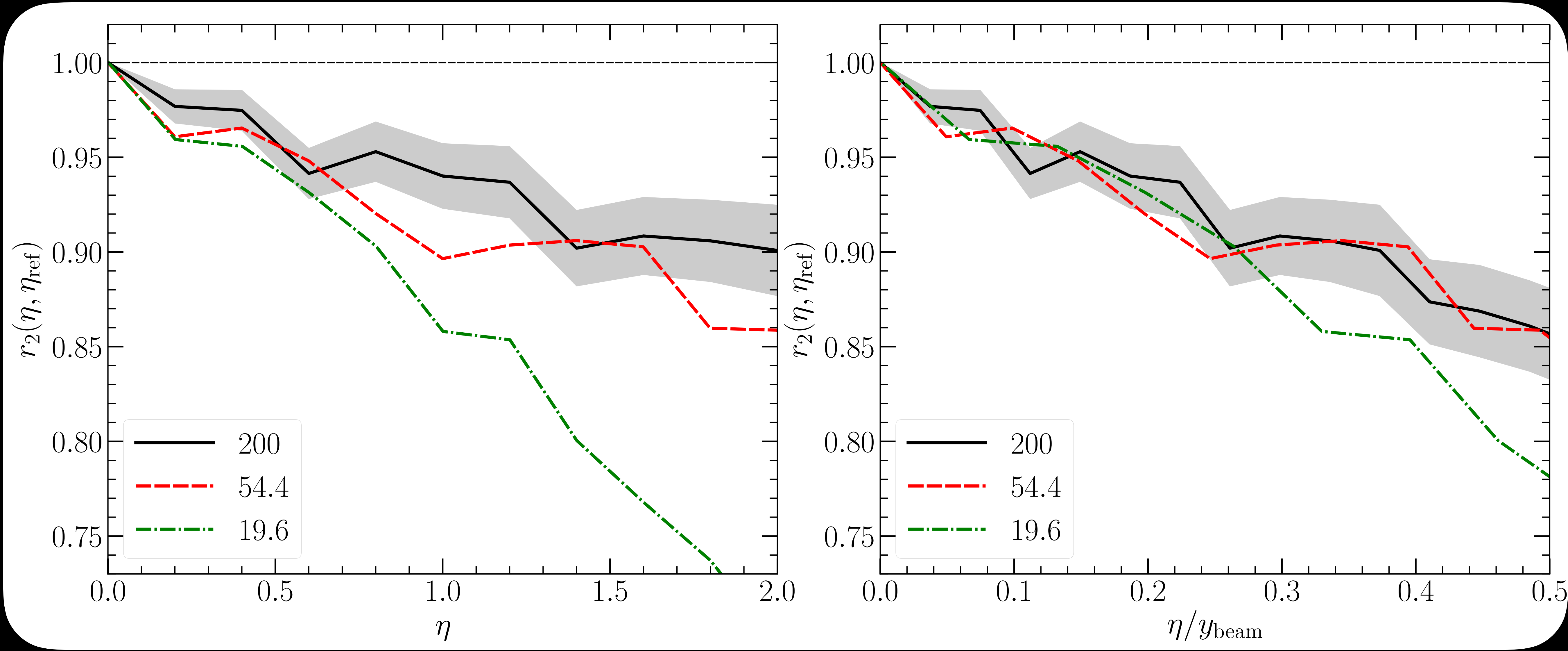

$$r_2(\eta, \eta_{\rm ref}) = \frac{\langle v_2(-\eta) v_2(\eta_{\rm ref}) \cos(2(\Psi_2(-\eta) - \Psi_2(\eta_{\rm ref}))\rangle}{\langle v_2(\eta) v_2(\eta_{\rm ref}) \cos(2(\Psi_2(\eta) - \Psi_2(\eta_{\rm ref}))\rangle}$$

- Longitudinal fluctuations imprint themselves on the event-plane decorrelation ratios; The r_n ratio decorrelates faster at lower energy